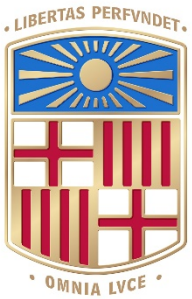

UNIVERSITAT DE BARCELONA

Final Degree Project

Biomedical Engineering Degree

"Optimization of SH-SY5Y Differentiation to Study Neuronal Mechanosensitivity"

Barcelona, 07 June, 2023

Author: Yara Hinojosa Grajales

Director/s: Jorge Oliver de la Cruz

Tutor: Pere Roca-Cusachs Soulere

Abstract

Neurodegenerative disorders, including Alzheimer's disease, pose a global social burden strongly linked with aging populations. Despite extensive research efforts, the underlying causes of the neuropathological changes that result in neuronal death are unknown, making the improvement of in vitro models a priority to address. Moreover, these pathological events are accompanied by alterations in brain rigidity, and while it is well established how various cell types can feel these mechanical cues and adapt their function, neuronal mechanosensing remains mostly unexplored.

For this reason, in this project we aimed to investigate the mechanobiology of Alzheimer's disease by optimizing the differentiation of SH-SY5Y cells into pseudo-neurons.

To facilitate neuronal differentiation, we adopted a novel strategy in which, by introducing a genetic construct in the SH-SY5Y cells, we could control the expression of the neuronal master gene NGN2. We demonstrated that this system, along with an optimized differentiation protocol, led to the production of more mature neuron-like cells.

Subsequently, the response of differentiated cells to mechanical stimulation was tested by culturing them in polyacrylamide gels with varying stiffness. Immunostaining and image analysis confirmed the morphological adaptation of neuron-like cells to matrix stiffness, presenting better morphology at a higher stiffness. Finally, we observed detectable levels of the co-transcriptional factor YAP and confirmed that its nuclear presence is mechanoregulated in neurons.

In conclusion, by combining differentiation techniques, genetic modification, and mechanical stimulation, our study provides a new model to explore Alzheimer's disease mechanobiology, potentially leading to innovative therapeutic strategies by uncovering complex underlying mechanisms.

Acknowledgements

First of all, I am pleased to express my sincere thanks to the director of this project, Jorge Oliver de la Cruz. His impeccable perseverance and dedication have been fundamental to the success of this work. I am deeply grateful to him for his extraordinary patience in the initial stages and his confidence in the final stages. Thanks to his guidance, I have gained the valuable knowledge that the world of research is based on experience and that there is always an approach to make things work.

I would also like to extend my gratitude to Professor Pere Roca for providing me with the opportunity to carry out this project within his esteemed research group, allowing me to learn first-hand about the fascinating field of cellular mechanobiology, particularly in its application to neurodegenerative diseases. To the members of Professor Pere Roca's team, I am thankful for the warm welcome and valuable advice they have provided. It is truly a pleasure to work alongside individuals who convey such enthusiasm for their work.

Lastly, I would like to express my heartfelt gratitude to my family and friends for their unwavering support and encouragement throughout this journey. Their presence and uplifting words have not only made this experience smoother but have also instilled in me a sense of enthusiasm and determination.

LIST OF FIGURES

LIST OF TABLES

GLOSARY

IBEC	Institute for Bioengineering of Catalonia
ECM	Extracellular matrix
PCB	Parc Científic de Barcelona
NGN2	Neurogenin2
WBS	Work Breakdown Structure
AD	Alzheimer's Diseases
APP	Amyloid-beta Precursor Protein
NDs	Neurodegenerative Diseases
TBI	Traumatic Brain Injury
FA	Focal Adhesions
ECM	Extracellular Matrix
YAP	Yes-Associated Protein
TAZ	WW domain-containing transcription regulator protein
3D	Three-Dimensional
iPSC	Induced Pluripotent Stem Cells
hPSC	Human Pluripotent Stem Cells
hiPSC	Human Induced Pluripotent Stem Cells
hESC	Human Embryonic Stem Cells
DOX	Doxycycline
rtTA	Reverse-Tetracycline Transactivator Protein
tetO	tet Operators
FBS	Fetal Bovine Serum
iFBS	inactivated Fetal Bovine Serum
RA	Retinoic Acid
BDNF	Brain Derived Neurotrophic Factor
KCl	Potassium Chloride
MAP2	Microtubule-associated protein 2
DCX	Doublecortin
NFs	Neurofilaments
NSE	Enrolase 2
PA	Polyacrylamide
DMEM	Dulbecco's Modified Eagle Medium
PBS	Phosphate Buffered Saline
UV	Ultraviolet
TEMED	Tetrametiletilendiamina
NF-H	Neurofilament-H
PERT	Program Evaluation and Review Technique

TABLE OF CONTENTS

1. INTRODUCTION

1.1. Cellular and molecular mechanobiology group (IBEC)

As we relate to our environment through incoming stimuli and transform this information into feedback, cells interact to their surroundings and respond accordingly. Of particular relevance is the mechanosensitive interaction, representing the reaction of cells to environmental forces, which determines how they proliferate, differentiate, and move; and regulates development, tumorigenesis or wound healing [1].

The "Cellular and molecular biomechanics" group, which belongs to the Institute for Bioengineering of Catalonia (IBEC) and is led by Pere Roca-Cusachs, seeks to unravel the molecular pathways that enable cells to sense and respond toward mechanical inputs, such as force or tissue stiffness, and how these stimuli trigger subsequent cellular responses. For this purpose, a combination of biophysical techniques such as magnetic and optical tweezers, atomic force microscopy, tensile microscopy and microfabricated force sensors with molecular biology, advanced optical microscopy and theoretical modelling are used.

It has been demonstrated that cells perceive beyond the stiffness exerted by the extracellular matrix (ECM), they also perceive interactions within other cells and even the composition and ligands embedded in the ECM. The membrane acts as a mechanosensor capable of detecting events nearby and even adapting itself if necessary. In fact, changes perceived externally can trigger nuclear modifications and affect the dynamics of transcriptional regulators in mechanotransduction processes. The goal of this group is to identify the molecular mechanisms that allow cells to communicate with their environment, in order to understand how these forces, influence the proper development of tissues and, on the other hand, tumour formation when this process is altered [2].

1.1.1. Installations

Located within the *Parc Científic de Barcelona* (PCB) facilities, IBEC benefits from a strategic location that provides access to shared resources and common facilities. In addition to IBEC's Core Facilities, researchers can also avail themselves of the PCB's centralized amenities, including freezers, ice machines, dark rooms, and white rooms. This integrated infrastructure further enhances the research capabilities and collaborative opportunities for scientists at IBEC, fostering a vibrant scientific community within the PCB ecosystem.

These interdisciplinary open lab spaces, distributed strategically, encourage collaboration and knowledge exchange among scientists with diverse expertise, promoting a dynamic research environment. Moreover, by sharing laboratory spaces, equipment, bench space, and benefiting from the support of qualified technical staff, researchers can conduct their work efficiently and effectively, while minimizing research costs.

The laboratory of Pere Roca's group is located specifically in the Helix building, which can be seen in Figure 1 below.

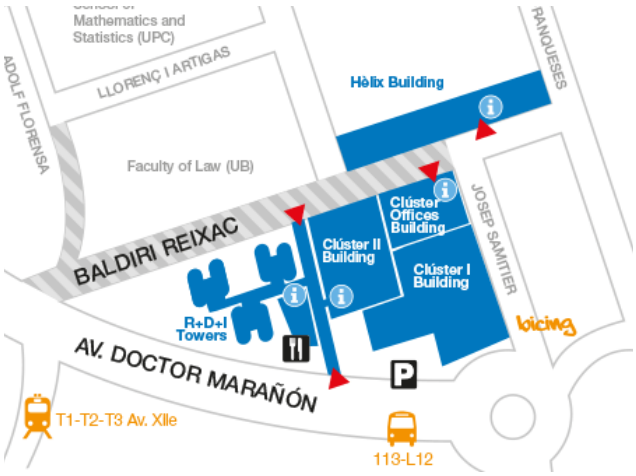

Figure 1. Facilities of PCB. Extracted from Adminpcb (2022)[3].

For this project, a selection of specific facilities and equipment within the group's available resources were utilized. These include tissue culture hoods, an optical microscope, offices, a confocal microscope, laminar flow hoods, laboratory bench areas, -80°C freezers, liquid nitrogen freezers, an ice machine, and the Infinite M200 PRO Multimode Microplate Reader from Tescan, all of them in Helix building. Furthermore, the PCB facilities for viral production were also used, these installations are located in the building called Cluster I.

1.2. Motivation

Throughout the development of my academic career, I have had the opportunity to attend courses related to biophysics and biomechanics, which has enabled me to acquire knowledge about the influence of mechanical stimuli from the environment on cells. This approach to study has been particularly fascinating for me and, consequently, has led me to become involved with the research line carried out by the group at the Institute for IBEC focusing on this topic.

My interest in the neuroscience field has also intensified over the years, particularly in relation to Alzheimer's disease. This condition, due to its high prevalence and the importance of prompt detection, has been a challenging field that has captured my attention, as an early diagnosis could mitigate the symptoms or, alternatively, improve the quality of life of those suffering from the disease. Thus, motivated by these experiences and personal concerns, I have decided to carry out a research project to study the use of neuron-like SH-SY5Y cells for Alzheimer's disease and its possible relation with mechanosensitivity in cooperation with Jorge Oliver de la Cruz, a postdoctoral researcher in Pere's group. This project intends to deepen our knowledge of this disease's mechanics and possibly contribute to the development of new study paths.

1.3. Objectives

The main objective of this study is to utilize the cellular model SH-SY5Y to develop a rapid differentiation method that generates enhanced neuron-like cells, surpassing the efficiency of current approaches through neurogenin2 (NGN2) overexpression. Additionally, the aim is to employ these neuron-like cells to assess their response to mechanical cues. This overall goal can be further divided into the following specific objectives:

- To demonstrate that the controlled induction of NGN2 expression via an inducible system enhances neuronal differentiation.
- To establish the mechanosensitivity of neuron-like cells by investigating their response to the stiffness of the surrounding environment.

Nevertheless, the project organization is as important as the conception idea; thus, it is essential to provide a detailed description of other objectives related to project management to ensure the success of the project:

- To develop a detailed project plan with specific objectives and deadlines for effective time management and achievement of the study objectives.
- To maintain regular communication with the project director to ensure coordination on study goals and progress.
- To ensure that the necessary resources are available to conduct the research project, such as laboratory materials, reagents, and equipment.
- To identify potential risks that could occur during the project and establish measures to mitigate them, for example, by conducting a guided tour of the laboratories and a risk prevention workshop.
- To incorporate measures that guarantee the accuracy and reliability of the study results, including the repetition of experiments and the utilization of feasibility study methods.

1.4. Limitations

It is anticipated that throughout the project, certain limitations related to process management or external factors may emerge, which could potentially affect its outcome and success. Hence, defining and considering such issues is crucial.

A major constraint is the short timeframe available to complete the study, with a maximum duration of 5 months. This time limitation implies that the research period is limited, and there may be restrictions on the number and complexity of experiments that can be feasibly implemented.

Another limitation to consider is the complexity of the laboratory methods and procedures involved. Although the director has previous experience in the topic and the techniques involved, it is still required to fine tune up the methods and procedures for this specific study. Similarly, although the

student has previous experience in the laboratory methodology, supplementary training may be required to master the techniques and procedures necessary to achieve the objectives stated.

In addition, there may also be limitations on the availability of necessary resources, such as laboratory materials, reagents, laboratory spaces, and equipment.

Finally, it is important to keep in mind that, due to the complexity of the subject, the outcomes from this project are inherently limited. Thus, further investigations will be necessary to validate and expand upon these findings.

1.5. Structure

This project has been divided into four fundamental blocks comprising all the activities undertaken, as illustrated in the flow chart presented in Figure 2.

Figure 2. Structure flowchart of the project.

Firstly, a comprehensive theoretical review of the project is conducted, which includes an extensive documentation process and assessment of the existing literature on the topic. This review will entail defining the theoretical framework of the project, the state of the art and situation of the current technology and market status. This block also involves identifying any applicable regulations and laws that may be relevant for the project, ensuring their consideration in the subsequent steps. This block is developed in sections 2, 3 and 9 of the present project.

The second block, outlined in sections 4, 6, 7 and 8, corresponds to conception engineering, where the specific steps will be defined, and the process will be elaborated in depth. Includes selecting the protocols to be employed and providing a comprehensive description of the materials and methods used. In addition, an execution schedule will be implemented, which includes the creation of a Work Breakdown Structure (WBS) and two graphs delineating the activity-time relationship. This section also addresses an assessment of the technical and economic feasibility of the project.

The third block, explained in section 5, is the detailed engineering and covers the thorough implementation of the selected solutions. This involves providing a detailed description of the obtained results and their analysis in the context of the topic.

Finally, the last block, in section 10, comprises the conclusions, where the implication and significance of the results will be discussed within the proposed theoretical framework. Furthermore, it will include a discussion of relevant future prospects and potential avenues for further research.

2. BACKGROUND

It is crucial to provide a theoretical framework for this project, which entails describing the fundamental aspects of Alzheimer's disease, including its typologies and symptoms. Additionally, it is important to investigate the current state of knowledge and research in this field, including the methodologies and technologies available for studying this disease.

2.1. General concepts

2.1.1. Alzheimer's Disease

Alzheimer's Diseases (AD) is one of the most common neurodegenerative illnesses. As the disease progresses, a person with it will develop severe memory impairment and lose the ability to carry out everyday tasks. Gradually, bodily functions are lost, ultimately leading to death. Currently, there is no cure, and the available palliative treatments are extremely limited [4]. At a cellular level, AD is characterized by loss of neurons and synapses in the cerebral cortex and certain subcortical regions. The neuronal atrophy and/or loss in AD are mainly attributed to:

i) **neurofibrillary tangles**, which consist of intraneuronal aggregates of TAU, the main microtubule associated protein in adult neurons. When hyperphosphorylated by several kinases, TAU loses the ability to assemble into microtubules and stabilization of the microtubule network, therefore disrupting neuronal cytoskeleton and precipitating into aggregates [5].

ii) **deposition plaques of extraneuronal toxic β-amyloid oligomers**, originated from the alternative cleavage of the amyloid-beta precursor protein (APP) by the β-secretase and γ-secretase. These pathological events are not exclusive of AD and can be also found in other neurodegenerative diseases (NDs) as well as in aged brains.

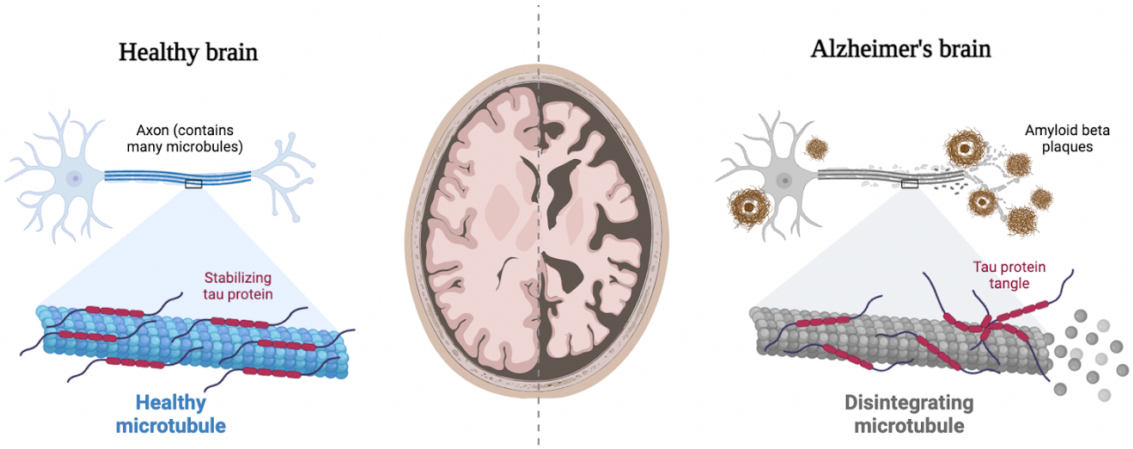

Figure 3. Representation of neurons in a healthy brain and neurons in an AD brain. Generated with www.biorender.com.

The cause of Alzheimer's disease is poorly understood, but it is considered a multigenic disease. Environmental risks identified by researchers include prolonged exposure to several heavy metals, particulate air, some pesticides, and traumatic brain injury (TBI). Currently TBI is probably considered the best-established risk factor for dementia: several meta-analyses have concluded that individuals who had a head injury of sufficient severity to result in loss of consciousness had an approximately 50% more risk of suffering dementia [6]. Nevertheless, the relation between mechanobiology and AD remains an unexplored avenue.

2.1.2. Cellular mechanobiology

Cells can sense environmental mechanical cues (mechanosensitivity) and integrate that information to adapt their function (mechanotransduction) by regulating critical cellular events, such as survival, differentiation, and proliferation. In order to feel and transmit forces, cells use Focal Adhesions (FA), which are multiprotein structures serving as mechanical linkage between the extracellular matrix (ECM) and intracellular cytoskeleton. The molecular composition of FA core is extremely variable and dynamic, responding to ECM composition and mechanics.

Intracellularly, the most studied mechanoregulated signalling corresponds to the Hippo pathway, which, in short, consists of a cascade of kinases that control the phosphorylation and nuclear activity of Yes-associated protein (YAP) and WW domain-containing transcription regulator protein 1 (TAZ). In conditions inducing low cellular tension, YAP/TAZ are phosphorylated and retained in the cytoplasm or degraded; otherwise, they can shuttle to the nucleus, where through the binding to transcription factor regulate the expression of important genes. This process is shown in Figure 4 below [7].

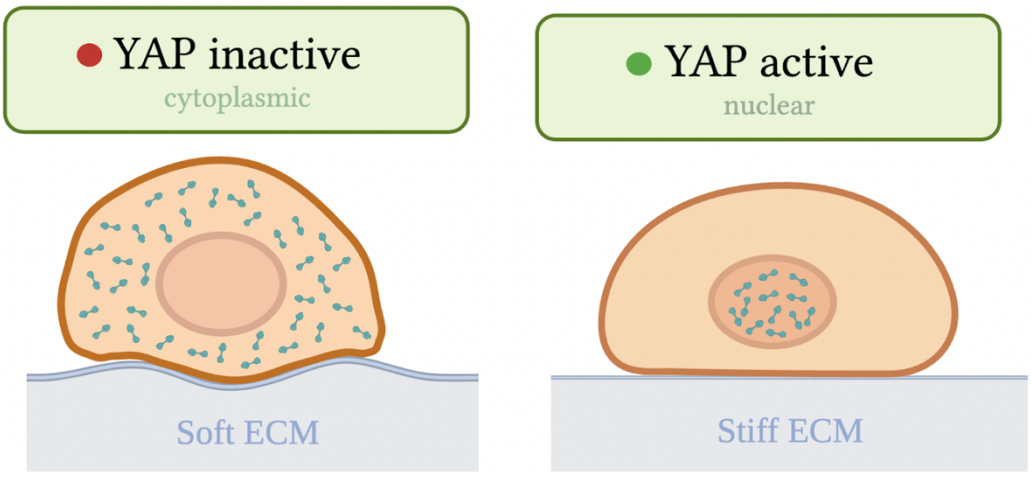

Figure 4. Simulation of YAP response to softer substrates where it is shown inactive, and stiffer substrates, where it is active and can be found in the nucleus. Generated with www.biorender.com.

2.1.3. Alzheimer and mechanobiology

While these mechanosensitive pathways are well characterized in other cell types, the neuronal-cell ECM interaction has been mostly neglected. This is mainly because neurons in the brain are mostly encompassed by synapses, astrocytic foot processes and other cellular structures; but they can still directly interact with the surrounding ECM. More importantly, the possible implication of mechanobiology in AD pathocellular events has not yet been explored. Deciphering the contribution of mechanobiology to neuronal physiology in disease will not only provide a new vision of AD and NDs in general but could also potentially identify new therapeutic targets that would revolutionize current treatments.

Neuromechanobiology, the intersection between mechanobiology and neuroscience, is still a young discipline. YAP and other Hippo components are known to play an important role in neural development as well as in neuronal survival and dendritic tree formation [8]. Oligodendrocyte progenitors [9] present a stiffness-dependent mechanoregulation of YAP nuclear activity similar to other cell types. Three-dimensional (3D) neuronal constructs have been also shown that neurons can partially respond to tissue stiffness and dimensionality, but the mechanism was not addressed [10].

Those are not the only evidence connecting mechanical inputs and AD. As exposed before, close-head TBI is probably considered the best-established risk factor for dementia [11], which according to the studies seems to apply shear strain to brain tissue [12] [13]. Moreover, direct and indirect estimation techniques have shown that brain stiffness is altered with aging [14] [15] and in several pathological conditions, including AD [8], Multiple Sclerosis [9], or stroke [16]. In addition, a lot of indirect evidence suggests an implication of mechanobiology in the development of AD. Although microtubular structures [17] and the activity of the TAU-associated kinase GSK3β [18] were found to be mechanosensitive, nothing has been described for changes in hyperphosphorylation, misfolding, and aggregation of TAU itself. Similarly, there are no studies about how tissue compliance affects the processing of APP protein into β- amyloid, but studies do show the cleavage of proteins following the same processing pathway [7] [19] [20].

The studies addressing the involvement of mechanosensing in NDs, and AD are very limited. In vitro models have focused mainly on the effects of biomechanics on axons and cell survival and/or glial activation [21] [22], but their impact in the appearance of neurodegenerative biomarkers was mostly ignored. YAP protein levels are altered in Huntington's disease patients [9]. A very recent study showed that the levels of nuclear YAP were decreased in neurons under early preclinical stages of AD pathology due to the sequestration into cytoplasmic β-Amyloid aggregates, thus suggesting that YAP-dependent neuronal necrosis represents a target for AD therapeutics [23].

2.2. State of the art

Initially, the research on AD predominantly relied on the examination of post-mortem brain tissue obtained from individuals affected by dementia. However, recent advancements in biomedical research methodologies have enabled scientists to replicate and study AD both in vitro and in vivo [24]. Therefore, experimental models play a crucial role in advancing our comprehension of the pathogenesis of AD and facilitating the preclinical evaluation of innovative therapeutic approaches. The main ones are presented in the current section.

2.2.1. Models to study AD

In vivo models

Transgenic mice have emerged as the predominant animal models employed in AD investigations, selected for their homologous anatomical structure to humans and easy manipulability. Nevertheless, other mammalian and invertebrate counterparts have also been used. Moreover, since the identification of genes implicated in AD, transgenic animal models have been generated through the integration of human mutant genes into the animal genome or the targeted removal of specific genes to mirror the pathological attributes of AD. However, these models incompletely recapitulate the entire gamut of AD's pathological traits, given their propensity to mimic only the genetic manifestations while eluding insights into sporadic AD cases. Conversely, non-transgenic animal models can be prompted to manifest AD-like symptoms, thereby enabling researchers to scrutinize not only the archetypal hallmarks of AD but also the intricacies of supplementary pathological mechanisms, encompassing oxidative stress, apoptosis, synaptic aberrations, neuroinflammation, perturbations in the gut microbiota-brain axis, and autophagy [25] [26].

In vitro models

Various cellular models have been devised to explore diverse facets of AD, encompassing primary cell cultures, cancer-derived cell lines, and induced pluripotent stem cells (iPSCs). Nonetheless, cell-based culture systems are unable to faithfully replicate the intricate environment of the human brain and the relation with non-neuronal cell populations, cell lines are more useful for perturbation experiments that aim to understand disease mechanisms at a cellular level [27].

The study of neurodegenerative disorders has been revolutionized by recent advancements in iPSC technology, addressing the challenge of limited access to living brain cells from patients. iPSCs, reprogrammed from mature somatic cells of both familial (FAD) and sporadic AD (SAD) individuals, offer the ability to differentiate into various cell types relevant to the disease while preserving the precise genome of the patient. To mitigate the inherent limitations of iPSC-derived two-dimensional (2D) cultures, the development of three-dimensional (3D) organoids has emerged. These complex self-organized aggregates, derived from iPSCs, consist of different cell types and closely emulate the intricate architecture of the brain [26].

Lately, 3D scaffold-based models of AD have been an object of great interest among researchers. These models offer the flexibility to select scaffold materials that align with the specific research question at hand. Matrigel, a widely used scaffold material, is particularly favoured for 3D neural cell cultures. However, it is important to acknowledge that many of these 3D models rely on in vitro induction of the AD phenotype, which may not faithfully replicate the intricate pathogenesis of the prevailing sporadic form of the disease. Further advancements are needed to improve the fidelity of these models in capturing the complex and elusive nature of sporadic AD [24].

2.3. State of the situation

Numerous approaches and methodologies have been utilized to explore neuronal characteristics and behaviours. Existing studies in this field provide valuable insights into the current state of knowledge, serving as benchmarks for understanding the intricate mechanisms underlying Alzheimer's pathology. This section aims to provide an overview of the existing research, especially regarding optimization of the model used and mechanosensitivity in the context of Alzheimer's disease.

2.3.1. Mechanobiology and AD articles

The close relationship between cellular behaviour and mechanostimulation is highlighting the significance of this discipline in cutting-edge research. However, due to its novelty, there are still limited articles available on the subject. This section will refer to two relevant articles in the field.

Hall et al. (2021) [28] states that the brain's neurons and glia express receptors that are known to be sensitive to mechanical stimuli. These receptors are activated by integrins, transmembrane cell adhesion molecules that establish a connection between the ECM and the cytoskeleton. Intriguingly, multiple studies have demonstrated that the inherent electrical properties of neurons can undergo changes in response to varying mechanical environments. The composition, structure, and stiffness of the ECM in the brain play a crucial role in the regulation of neuronal and glial function. Consequently, alterations in the composition and stiffness of the ECM that occur with aging and neuropathological conditions can disrupt the mechanosensitivity of neurons and glial cells, potentially contributing to the progression of neurodegenerative diseases. However, our current comprehension of how the mechanical characteristics of the brain evolve during aging or in the presence of neuropathologies like AD remains somewhat limited due to certain experimental and technical challenges.

Comparatively, neurodegenerative disorders like Alzheimer's disease are likely to induce more pronounced perturbations in brain mechanobiology than the natural aging process. Notably, amyloid plaques, a characteristic feature of Alzheimer's disease, possess a higher degree of stiffness than their surrounding environment. This heightened stiffness of the plaques, summed to

the lowering of neurons and glial cells density, contributes to an overall softening of the macroscopic properties observed in the Alzheimer's disease-afflicted brain.

Another article, Tortorella et al. (2022) [29], affirm that astrocytes respond to mechanical stimuli from amyloid plaques by potentially influencing neuroinflammatory responses. Moreover, the Hippo pathway, particularly the effector YAP, shows downregulation in AD, contributing to amyloid plaques formation and tau hyperphosphorylation. Also, cell adhesion molecules expression is altered in AD, impacting neuroinflammation and amyloid metabolism. These mechanobiology alterations have implications for AD pathogenesis and provide potential avenues for therapeutic intervention.

2.3.2. SH-SY5Y cell line

The SH-SY5Y cell line, derived from human neuroblastoma, is widely utilized in research focusing on neurotoxicity, oxidative stress, and neurodegenerative diseases. Research has indicated that undifferentiated SH-SY5Y cells express markers characteristic of immature neurons and lack markers associated with mature neurons. As a result, the undifferentiated SH-SY5Y cell line may not be a suitable model for diseases like Parkinson's disease, which predominantly affect fully differentiated dopaminergic neurons. Thus, SH-SY5Y cells can be differentiated into mature neurons using various substances. While there are some observations that question their neuronal maturity, such as moderate dendritic outgrowth and lack of spontaneous activity, they express markers of neuronal maturation and exhibit excitability, synaptic formation, and axonal outgrowth. Overall, there is strong evidence supporting the neuronal maturity and functionality of SH-SY5Y-derived neurons [27] [30].

2.3.3. NGN2-Dox Complex

Human pluripotent stem cells (hPSCs) have emerged as a valuable alternative to rodent models and established cell lines for studying neurodevelopment and neurodegeneration. These cells offer a more accurate representation of human neurobiology, overcoming inherent genomic disparities and variations in neuronal subtypes. Utilizing hPSCs differentiated into neurons enables researchers to generate and investigate human-derived neuronal populations, contributing to a deeper understanding of these processes. Differentiation protocols that rely on external factors have drawbacks in terms of their limited ability to consistently produce mature and functional neurons, often resulting in low yields and requiring substantial time and resources. In contrast, the controlled activation of specific transcription factors allows for the rapid generation of functional neurons from various cell sources such as progenitors, stem cells, and fibroblasts. This approach significantly accelerates the process compared to traditional methods that rely on external factors for differentiation.

Neurogenin2 is responsible for encoding a transcription factor specific to the nervous system called NGN2, which has the ability to trigger the development of neurons in both somatic cells and stem cells. NGN2 is expressed in neural progenitors during the formation of the central and peripheral nervous systems. Studies have shown that introducing an excess of NGN2 into human induced pluripotent stem cells (hiPSCs) or human embryonic stem cells (hESC) effectively prompts their transformation into neuronal cells [31] [32].

In order to study the outcomes of specific genes in SH-SY5Y cells (such as NGN2), it is crucial to have precise control over their expression levels at different time points. Researchers have developed artificial gene expression systems that allow for regulated and reversible control of gene activity using safe and non-toxic molecules. The TetON system, a widely utilized gene regulation system, employs the antibiotic doxycycline (dox) to achieve its effects. When doxycycline is present, it binds to the reverse-tetracycline transactivator protein (rtTA), inducing a conformational change. This alteration enables the rtTA to selectively interact with specific DNA sequences called tet operators (tetO) situated in the promoter region of the target gene. Consequently, this binding event triggers the activation of gene expression by facilitating the recruitment of cellular machinery responsible for transcription [33]. These gene regulation systems provide researchers with valuable tools to precisely control gene expression in SH-SY5Y cells, allowing for the investigation of various biological processes and disease mechanisms [34].

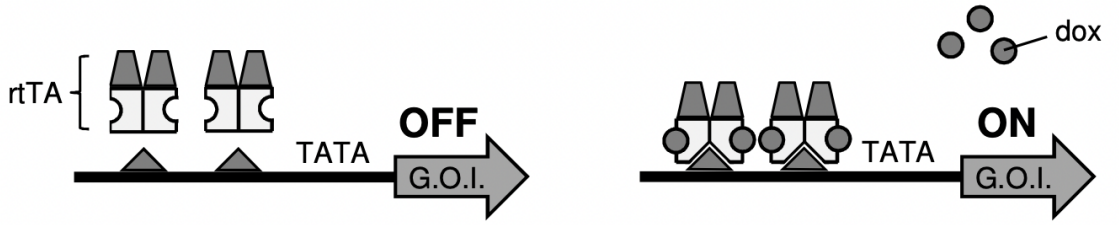

Figure 5. Representation of the Tet-ON system. As can be seen, in absence of doxycycline the rtTA is not bound to tetO, and when doxycycline appears it binds and the Gene of interest (G.O.I.) starts transcribing thanks to TATA sequence. Extracted from Das, Tenenbaum and Berkhout (2016) [35].

If this system is employed with the gene of interest being NGN2, it would provide the researcher with the capability to selectively activate the transcription of neurogenin2 according to their discretion.

3. MARKET ANALYSIS

In 2019 Alzheimer's disease constituted approximately 70% of all dementia cases, had a global prevalence of 55 million (M) and an estimated global societal cost of US$1.3 trillion. Nevertheless, it is projected that by 2050, the prevalence will reach 139M individuals worldwide, primarily due to population aging [36]. This demographic shift highlights the need for substantial resources to adequately care for patients with AD. To address this growing concern, ongoing research aims to develop interventions to delay disease onset and slow its progression [37]. Various treatments to

slow disease progression and prevention strategies, including lifestyle changes, are currently being investigated. These effective interventions have the potential to significantly reduce the prevalence and incidence of Alzheimer's disease, improve the quality of life for patients and caregivers, and alleviate the burden on healthcare systems. Collaborative research initiatives, the focus of market players on launching new drugs, and the increasing incidence of central nervous system disorders are contributing to the expansion of the market. Furthermore, advancements in treatment approaches, drug discovery techniques, and a robust pipeline of potential therapies offer significant growth opportunities [38] [39] [40].

3.1. Historical Market Evolution

Dementia, an age-related neurological disorder, has a complex history with several notable milestones. In about 2000 B.C., the ancient Egyptians recognized that memory declines with age. During the Middle Ages, mental illnesses like dementia were believed to be divine punishments, leading to the persecution, and burning of individuals, especially women, during witch hunts. In 1797, Philippe Pinel accepted dementia as a medical term, and later, Dr. Alois Alzheimer's clinicopathological studied of Auguste D. and provided crucial insights of the disease. This led to the official naming of "Alzheimer's disease" and the development of diagnostic techniques, genetic discoveries, and therapeutic interventions. Advancements in brain imaging, biomarker analysis, and new technologies have improved our understanding and paved the way for potential treatments in the future. Ongoing research focuses on immunotherapies, gene therapies, and other innovative approaches to combat this challenging condition and enhance the lives of individuals affected by dementia [41] [42].

3.2. Future Market Perspectives

Efforts to find effective treatments for Alzheimer's disease face several challenges, including incomplete understanding of AD pathogenesis, complex disease etiology, slow disease progression, and comorbidities in the elderly population. Global leaders have set a deadline of 2025 to address these challenges and develop innovative diagnostic tools and prevention strategies. Early detection is crucial as symptoms appear only in advanced stages of the disease. Precision medicine approaches aim to personalize treatment based on genetic, neuroimaging, biochemical, and neuropsychological profiles. Ongoing research focuses on diverse therapeutic targets, including neurochemicals, amyloid and tau pathology, inflammation, mitochondria, and lifestyle interventions. Successful outcomes in these areas hold promise for effective AD treatments and prevention strategies [43] [44].

4. CONCEPT ENGINEERING

During this stage, an exhaustive analysis is conducted to explore various solutions, considering alternative approaches, and carefully evaluating their suitability and feasibility. This involves a systematic examination of different possibilities, weighing their merits and drawbacks, and finally choosing the solution that is going to be implemented.

4.1. Study of solutions

It is crucial to consider that in a scientific study of this magnitude, there are procedures and components that do not allow for changes, such as experimental protocols or the available machinery. However, the study of solutions encompasses certain processes that can be customized or selected, and it is in this section where they are described and examined in order to choose the best option.

4.1.1. Model

A thorough assessment of the state of the art has been done, with a particular focus on the many models used to investigate Alzheimer's disease. To be able to select the option most suitable for the study, it is necessary to carefully evaluate the benefits and disadvantages of each type. The Table 1 below presents the analysis's distilled conclusions.

Table 1. Advantages and drawbacks of the main models to study AD.

MODEL	BENEFITS	DRAWBACKS
ANIMAL MODELS [45] [46] [47]	Ability to study complex physiological and behavioral responses. Similarities to human biology, allowing better translation.	Ethical considerations regarding animal experimentation. Costly and time-consuming experiments. Variability between individuals and species.
CELLULAR MODELS [48]	Controlled and reproducible experimental conditions. Potential for high-throughput analysis. Cost-effective and less time-consuming experiments.	Simplified representation of complex biological systems. Lack of in vivo complexity and physiological relevance.
hiPSM [48] [49]	Ability to derive patient-specific neurons for personalized research. Potential to study disease mechanisms and test therapeutic interventions.	Complex and time-consuming cell reprogramming process. Variability in differentiation protocols. Limited maturity and functionality of hiPSC-derived neurons.
3D MODELS [48]	The most similar approach to reality. They can even simulate brain regions and the synapse between them.	Require more protocols, time, and money. They are still an immature technique. Very complex to achieve and standardize.

Animal models have proven valuable for studying the physiological effects of drugs. However, their ability to accurately replicate the exact conditions of the human brain is hindered by inherent

physiological and genetic disparities. Additionally, the maintenance and study of animals necessitate additional time and attention.

Human induced pluripotent stem cell models offer a specialized approach for researching neurological illnesses and the chance to look at highly differentiated human neurons. However, reprogramming iPSCs is a complicated procedure that can be difficult, especially for those who are new to the field, like undergraduates. Furthermore, compared to other cellular models, the delicate nature of the obtained cells needs precise handling and prolonged cultivation times.

On the contrary, three-dimensional models can accurately emulate physiological phenomena in the body, encompassing intercellular interactions, cellular connectivity, and holistic dynamics. Nevertheless, as a young technology, it is currently in transition, lacking in stability, and requiring significant investments in terms of both time and money. Furthermore, it remains challenging to achieve the ideal outcomes in 3D models as a result of the complexity involved.

Ultimately, cellular models exhibit a high availability, and, despite their simplified portrayal of the intricate human physiology, they provide a path for conducting high-throughput investigations. Moreover, their cost-effectiveness and streamlined manipulation offer significant advantages over alternative models. Given the timeline and the comparative ease of implementation associated with cellular models, they have emerged as the preferred solution.

Once decided to employ a cellular model, the following step involves selecting the most suitable option. Considering factors such as their widespread accessibility, ease of maintenance, and the existence of well-established protocols for experimental procedures, cell lines have been selected as the preferred choice. However, in order to determine the specific cell line to use, an examination of the main ones employed in AD research has been undertaken. The following table, adapted from Dubey et al. (2019b) [48], provides a concise description of various cell lines for AD studies.

Table 2. Specifications of three cell lines used for AD research.

Cell line	*Description*
HEK293 (Human embryonic kidney cell 293)	Non-neuronal but express neuro-filament subunits and Tau-protein. Useful to study of τ-protein phosphorylation and neurodegeneration
SHSY-5Y (human neuroblastoma cell)	Tumorous cells that resemble neurons after differentiation. Useful to study the mechanisms of AD, to investigate the relationship between AD glucose metabolism and to study oxidative stress, neurotoxicity, and neurodegeneration process.
PC-2 cell line (pheochromocytoma cell line)	When differentiated resemble sympathetic ganglion neurons. Used for neurite growth or differentiation into nerve like cell and to study of different pathway.

The **SH-SY5Y cell line** has been determined to be the most suitable for investigating neuronal differentiation and analysing protein expression in response to gel stiffness among the three cell lines mentioned above. This choice is based on several methodological and biological factors. Firstly, SH-SY5Y cells are derived from human neuroblastoma tissue, which facilitates their differentiation towards the neuronal phenotype. In contrast, HEK293 cells originate from human embryonic kidney tissue and, although they display some neuronal proteins such as tau and neurofilaments, they do not effectively differentiate into neurons. Similarly, PC-2 cells, derived from human glioma tissue, differentiate preferentially into glial-like cells rather than neurons.

4.1.2. SH-SY5Y differentiation

It has been recognised that these cells in their undifferentiated state lack the distinctive morphology, functional properties and gene expression patterns associated with mature neurons. To bridge this gap and create a more accurate representation of mature neurons, researchers employ various differentiation protocols to induce maturation of SH-SY5Y cells by applying specific differentiation factors and signalling pathways.

During the differentiation process, undifferentiated SH-SY5Y cells undergo morphological changes, accompanied by alterations in gene expression, with overexpression of mature neuronal markers and underexpression of progenitor cell markers. Hereafter, it is pertinent to acknowledge and evaluate specific protocols for potential utilization, in the present section we analyse two established methodologies:

Dravid et al. (2021) protocol [50]

The differentiation technique used in this study combines two previously established protocols, incorporating certain modifications based on the recommendations provided by each method. Initially, undifferentiated cells are cultured in basic growth medium for a defined period to establish a suitable cellular environment before initiating the differentiation process. Subsequently, the cells are seeded onto Matrigel-coated dishes to facilitate adherence and improve differentiation efficiency. The next step involves transitioning the cells to stage 1 medium, which contains a lower amount of Fetal Bovine serum (FBS) and Retinoic Acid (RA) for 5 days. After this period, the cells are exposed to stage 2 medium, containing Brain Derived Neurotrophic Factor (BDNF) and Potassium chloride (KCl) in a Neurobasal-B27 mixture, for another five days. After a total duration of 10 days, the cells are considered to have successfully undergone differentiation and acquired a pseudo-neuronal phenotype. At this stage, the differentiated cells can be used for research purposes, serving as a valuable model system for studying neuronal properties and conducting various investigations.

Overbaugh, Mangold and Szpara (2016) protocol [51]

The method incorporates previous techniques and starts with a sequential removal of serum from the culture media and addition of RA. This gradual deprivation of serum is followed by introducing

extracellular matrix proteins and neurotrophic factors, which leads to a selective and homogeneous differentiation towards neuronal phenotype. The differentiation protocol spans a total of 18 days and consists of 11 sequential steps. From day 0 to 7, the cells are coated with Medium #1. On day 7, the cells are split 1:1 onto uncoated dishes with Differentiation Medium #1. On day 8, the media is switched to Differentiation Media #2, and on day 10, the cells are split again onto ECM-coated dishes in Differentiation Media #2. From day 11 until day 18, cells are incubated in Medium #3. At day 18, the differentiated neurons are ready for downstream applications.

The two procedures are both useful for differentiating SH-SY5Y cells into neurons and preparing them for further use. However, the procedure described by Overbaugh, Mangold and Szpara is more complex, requiring an additional time of 8 days, cell passaging and the use of three different media. In contrast, the procedure described by Dravid et al. is more convenient due to the availability of the necessary components in our laboratory, its shorter duration and ease of the procedure. For these reasons, it has been decided to follow the procedure proposed by **Dravid et al.**

Nevertheless, both procedures still present some issues that could be limiting and that can be further improved. One of the main drivers of the first part of neuronal induction in both protocols is all-trans retinoic acid. This molecule is photounstable and cannot be stored for long periods, therefore requires the preparation of new stock for each differentiation. To overcome this issue, synthetic analogs have been developed, such as EC23. It is a photostable molecule that has been proved able to induce neural differentiation of human pluripotent stem cells and the cell line ReNcell 197VM [52] [53].

Another problem that affects ulterior analysis is cellular detachment during differentiation. While having a reduced proliferation rate under the differentiation conditions, SH-SY5Y neuron-like number slowly increases over time in the culture plate. Moreover, as the cells differentiate, they generate an intricate network of cellular connections. As a result, a monolayer is formed that can be easily detached as a whole during regular media changing. To overcome this problem, the addition of laminin to the cell culture media has been shown to promote cellular attachment and enhance matrix deposition during neuronal differentiation [54].

In hiPSCs, the controlled expression of Neurogenin2 can induce the fast differentiation of the stem cells into neurons (For more information see section 2.3.3.). Therefore, the usage of the construct NGN2 induced by doxycycline is going to be used to prove it enhances differentiation in SH-SY5Y cells.

4.1.3. Evaluation of cell differentiation

4.1.3.1. Cell viability

The study of cell viability—the proportion of healthy cells in a sample—can be a helpful factor to determine if different concentrations of doxycycline can affect the survival rate of cells, specifically of SH-SY5Y cells. Therefore, by selecting the optimum concentration of DOX, the project outcomes can be more satisfactory.

Currently, two methods are being mainly used in Pere Roca's group, PrestoBlue and MTT. The MTT assay involves incubating cells with MTT solution, which is then transformed into purple formazan crystals by active enzymes in viable cells. The crystals are dissolved, and the absorbance is measured. PrestoBlue assays are conducted in plates, where cells are incubated with the respective solution, and the change in fluorescence is measured. In comparison, PrestoBlue offers several advantages over MTT. Firstly, PrestoBlue is claimed to be a faster assay, with the ability to assess cell viability within 10 minutes of incubation, compared to the 3-hour incubation required for MTT. Secondly, PrestoBlue is more sensitive, being able to detect as few as 12 cells, while MTT requires a higher number of cells for detection. Furthermore, it is not significantly affected by the plate color, reading mode, and storage of plates for up to 7 days, and this flexibility and convenience make PrestoBlue a practical choice for researchers. Additionally, it is soluble in culture media and non-toxic to cells, allowing the assayed cells to be used in subsequent tests. In contrast, MTT assay kills the cells by forming crystals and can only be used as an end-point procedure.

In summary, **PrestoBlue** offers advantages over MTT in terms of sensitivity, speed, and cell viability preservation so it is concluded to be the more suitable choice for assessing cell viability in the present project [55].

4.1.3.2. Neuronal markers detection

First, we wanted to assess which neuronal markers we wanted to investigate in order to evaluate differentiation. Given the abundance of proteins assessed in similar investigations, a comprehensive analysis was conducted to determine the most commonly studied markers. The subsequent table presents a detailed description of these selected markers.

Table 3. Description of neuronal proteins.

Neuronal Protein	***Description***
Microtubule-associated protein 2 (MAP-2)	Neuron-specific cytoskeletal protein expressed in the nervous system of embryonic and adult tissues; it is used as a marker of neuronal phenotype. Considered a marker for mature neurons [56].
Doublecortin (DCX)	Marker of neurogenesis in the central nervous system, it is expressed by migrating neurons and can be observed at the beginning stages of neuronal development [57].
β-III Tubulin	Expressed during neuron early-stages, is a build block of microtubules, an important component in the cytoskeleton. Is considered a marker for immature neurons [58].
Neurofilaments (NFs)	Neurofilaments belong to the intermediate filament family of proteins and provide structural support and maintenance of axon calibre. NFs are primarily composed of three subunits; neurofilament light (NF-L), medium (NF-M), and heavy (NF-H) [59].
Tau	Modulates stability of the cytoskeleton and provides axonal flexibility, it is found in distal portions of axons. It is a marker of neurodegenerative disorders, especially AD [61].
Ennolase 2 (NSE)	Brain-specific glycolytic enzyme that is involved in intracellular energy metabolism. NSE levels increase during maturation of the cell [62].

The proteins featured in the table exhibit varying degrees of informational utility, contingent upon their specific functional roles. In alignment with the aims and objectives of the present study, a thorough evaluation has led to the estimation that **NFs, MAP-2, βIII-tubulin**, and **tau** proteins represent the most pertinent candidates for tracking purposes. In addition to the aforementioned proteins, two additional proteins have been included in this study due to their significance in advancing our understanding of the cellular processes under investigation. **Yap**, known for its involvement in mechanobiological mechanisms within cells, has been included to explore its potential impact on the observed phenomena. Moreover, the assessment of neurogenin2 presence within cells serves as a valuable indicator of the efficacy of our experimental approach of adding **NGN2** to the differentiation process.

Finally, to further study the neuronal markers present inside the neuron-like cells in order to evaluate the success of differentiation we need to search for a method. Two possible options arise since they are disponible inside the lab.

Real time PCR is “a recent modification to the polymerase chain reaction that allows precise quantification of specific nucleic acids in a complex mixture by fluorescent detection of labelled PCR products” according to Fraga et al. (2008) [63]. Real-time PCR offers significant advantages in neuronal marker analysis. It provides extreme sensitivity, enabling the detection of even low levels of gene expression. The process is highly automated, making it quick and efficient. Moreover, a lot of different markers can be analysed in one sample [64]. However, sometimes low volumes and the presence of PCR inhibitors are a problem.

Immunocytochemistry, on the other hand, refers to “The use of antibodies to localize structures in cell cultures and tissue sections", affirms Burry (2011) [65]. It enables the visualization of multiple intracellular antigens simultaneously and allows to visualize their localization in the cell. Furthermore, when coupled with confocal microscopy, it eliminates the need for embedding and sectioning, preserving antigens and improving antibody accessibility.

Immunocytochemistry has been chosen as the preferred methodology for its capability to visualize the intracellular distribution of proteins. In the context of neuronal research, this information assumes great significance due to the contextual variations observed for proteins in distinct cellular compartments. Notably, proteins localized within the soma or axons of neurons can convey fundamentally different functional implications, thereby highlighting the criticality of discerning their spatial organization for comprehensive understanding.

4.1.4. Hydrogel selection for mechanobiology studies

In the realm of mechanical studies involving neuron-like cells, the choice of gel substrate plays a pivotal role in achieving an optimal environment for probing mechanosensitive properties. An extensive array of gel options is available, both through laboratory fabrication and commercial procurement. Among these options are Polydimethylsiloxane, Polystyrene gels, Polyethylene glycol hydrogels, and Polyacrylamide (PA) gels. After careful consideration, our research has led us to select **Polyacrylamide** as the gel substrate of choice due to its numerous advantages.

Polyacrylamide offers a well-established technique within our laboratory, supported by a protocol followed by many researchers. The mentioned protocol provides the ability to be fabricated with a wide range of stiffness, and therefore precisely control the mechanical properties of the gel substrate. Furthermore, studies have demonstrated the compatibility of PA with SH-SY5Y cells and with subsequent analyses, such as confocal imaging [66]. Lastly, it allows functionalization with a diverse range of proteins, allowing for the exploration of specific molecular interactions and signalling pathways within the context of our study.

The determination of appropriate gel stiffness is a crucial consideration in mechanobiological studies utilizing PA gels. In this regard, extensive discussions have taken place regarding the optimal stiffness range, leading to the selection of **30 kPa** and **1.5 kPa** as suitable values since it is widely acknowledged that the majority of mechanosensitive cells exhibit distinct responses within that stiffness range. Moreover, previous investigations have revealed notable differences in the neuronal differentiation of SH-SY5Y cells within this stiffness range [66].

These gels are going to be coated in laminin for better adhesion. The selection of laminin as the protein coating for gel substrates in this study is based on its adhesive properties and its relevance to neuronal differentiation. Laminin, an adhesive glycoprotein similar to fibronectin, plays a crucial role in the extracellular matrix (ECM) and is abundant in Matrigel [67]. In this experimental context,

laminin is utilized to enhance cell adhesion during neuronal differentiation. By harnessing the adhesive characteristics of laminin, the aim is to establish an environment that fosters cell-substrate interactions and facilitates the differentiation of neuronal cells.

4.1.5. Evaluation of mechanosensitivity

In the field of mechanosensitivity evaluation, several methods have been proposed to assess cellular responses to mechanical stimuli. Among these methods, **mechanotransducers** have emerged as a promising approach to unravel the mechanosensitive nature of cells. Three potential mechanotransducer candidates that were considered include Piezo channels, focal adhesions involving integrin-vinculin-talin complexes, and the YAP (Yes-associated protein) pathway. After careful deliberation, the decision was made to focus on the Hippo effector **YAP** due to its extensive scientific literature supporting its role as a highly regulated mechanotransductior and its robustness and well-established readout through the assessment of nuclear-cytoplasmic ratio (see Figure 4). By describing YAP behaviour, our study aims to contribute to the expanding understanding of mechanosensitive cellular responses in a formal and scientific context [68] [69].

Again, to visualize YAP, immunocytochemistry and confocal microscopy will be used as it provides the possibility to visualize the location of the protein, a useful tool for this specific protein.

4.1.5.1. Image analysis software

To analyse the acquired images obtained as experimental outcomes, several programs can be employed, with the most renowned ones being ImageJ and CellProfiler, which are widely utilized open-source platforms, with a strong presence in the scientific community. ImageJ is favoured for interactive, single-image processing, while CellProfiler shines in project building and automation [70]. Both are indispensable tools in the field of biological image analysis. CellProfiler offers a flexible platform for automating image analysis, addressing a wide range of biological questions. It eliminates the tedium of repetitive visual analysis, producing rapid and accurate results [71]. Meanwhile, ImageJ serves as an essential tool for routine image processing and analysis, providing a comprehensive range of import filters, a suite of processing and analysis routines, and enthusiastic support from a friendly mailing list [72]. Although both ImageJ and CellProfiler offer valuable features, our selection for this particular project is ImageJ, primarily due to the student's prior familiarity with the software, and also because several tools and scripts can be found already tested and developed to calculate the nuclear-cytoplasmic ratio. For example, the Intensity Ratio Nuclei: Cytoplasm Tool (RRID: SCR_018573) can be a useful tool for evaluating YAP subcellular distribution.

4.2. Final Solution

The following section provides a detailed account of the proposed solution for the methods employed in this project. In Figure 6 below a workflow of the steps of the project is represented.

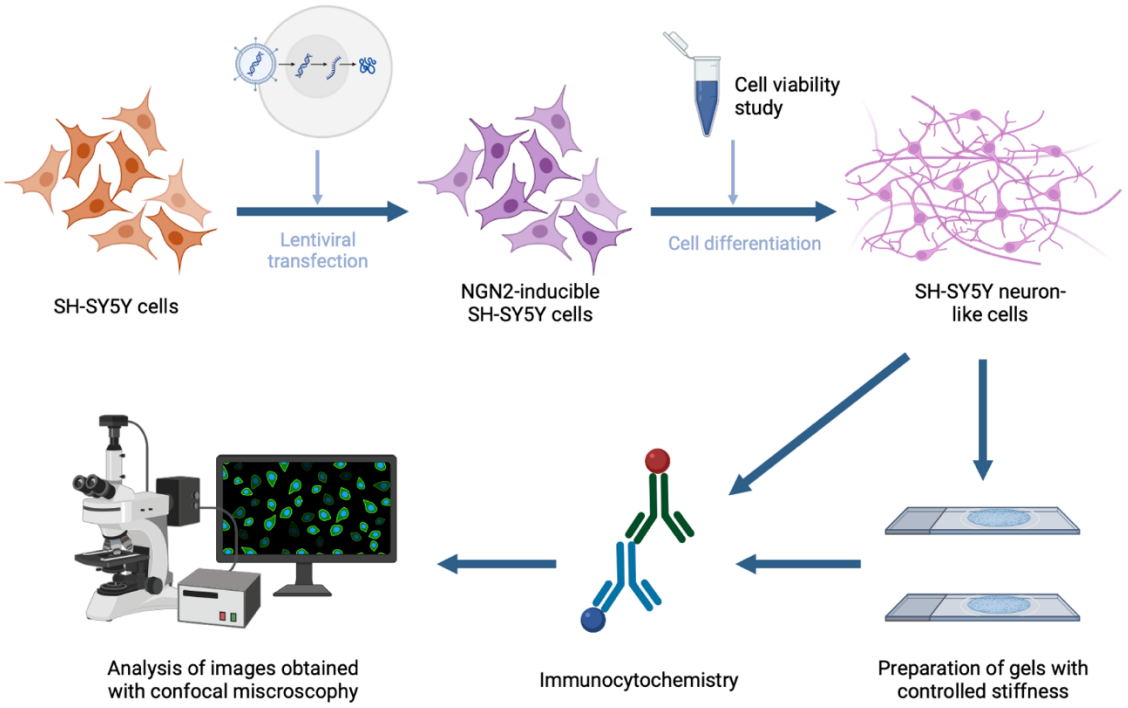

Figure 6. Workflow of the solution followed for the project. Generated with www.biorender.com.

The initial step of this investigation involves the cryopreservation of the obtained cells for subsequent storage until their intended utilization. Subsequently, upon initiation of the experimental procedures, the cells will undergo thawing and be partitioned into two distinct cohorts: SH-SY5Y cells and SH-SY5Y cells subjected to transfection with lentivirus containing the NGN2 gene to obtain a DOX-inducible model. Following this, a process of cellular differentiation will be conducted on both groups to assess the impact of doxycycline-induced gene activation on the attainment of heightened neuronal differentiation. Once differentiated into pseudo neurons, a subset of the cells will undergo an immunocytochemistry, while the remaining cells will be seeded onto prefabricated gels possessing controlled stiffness properties, specifically 30 kPa and 1.5 kPa, to scrutinize the behavioural responses of pseudo-neuronal entities. After appropriate fixation, immunocytochemical procedures will be performed. The immunostained images will be acquired using confocal microscopy and then subjected to analysis employing ImageJ software. The methods and procedures are detailed below.

4.2.1. SH-SY5Y culture

The SH-SY5Y cell line was a kind gift from Dr. Pozo-Devoto (Brno, Czech Republic). Cells will be expanded by culturing them in 75 cm² culture flasks. The culture and handling of the cells requires

an environment with controlled conditions that mimic the characteristics of the human intracellular environment.

To initiate the culture, it is necessary to supplement cells with specific substances that will provide the necessary nutrients, therefore, the medium will be formed by DMEM/F12, FBS inactivated and Pen/Strep*L-Glut. This formulation provides a wide range of nutrients, vitamins, and minerals essential for cell growth and maintenance. Inactivated FBS contains growth factors, hormones and other essential components that promote cell proliferation, survival, and growth. Inactivation of FBS is carried out to prevent the action of complement components and to avoid contamination by mycoplasmas. Finally, Penicillin-Streptomycin (Pen/Strep) antibiotics are added to the medium to keep the culture free of bacterial contamination, thus preventing the proliferation of undesirable microorganisms. In addition, L-Glutamine, an essential amino acid, is included in the medium to support cell metabolism and growth.

Once the culture medium has been obtained, the cells shall be suspended for seeding. In the case of frozen cells, thaw by immersing the cryovial in a 37°C water bath, carefully clean with 70% ethanol, dilute the contents of the cryovial in 6 ml of warm medium, centrifuge and resuspend in 1 mL of medium. Alternatively, if the cells are from a plate or flask, they shall be washed with PBS for 5 minutes before TrypLE™ is added and left to incubate in the incubator for a further 5 minutes. Once detached, cells shall be collected in a tube and centrifuged, then resuspended in 1 mL of medium. After the cells are suspended, they will be reseeded in a proportion 1:20 in a new 75 cm² culture flask containing 15 mL of medium. The cells shall adhere to the bottom of the flask and begin to proliferate. To ensure adequate nutrition, the medium should be changed every 2-3 days. As the cells multiply and reach around 90% of confluence, around one week later, the cell passage procedure is repeated to transfer the cells to a new flask, thus ensuring optimal growth and avoiding overpopulation in the current flask (for complete protocols and more detailed information, please refer to Annex 1).

4.2.2. Lentiviral transfection and production of the NGN2-inducible cell line

A fraction of SH-SY5Y cells will be subsequently infected with the lentivirus carrying the inducible system able to control the expression of NGN2 gene upon the inclusion of doxycycline in the medium, infected cells will serve as a control to compare the performance of the infected cells. This comparison allows us to assess whether the presence of the NGN2 gene results in improvement or deterioration in the results obtained, and thus prove or disprove our hypothesis. The cell infection procedure using the lentivirus is detailed below, and a workflow can be observed in Figure 7.

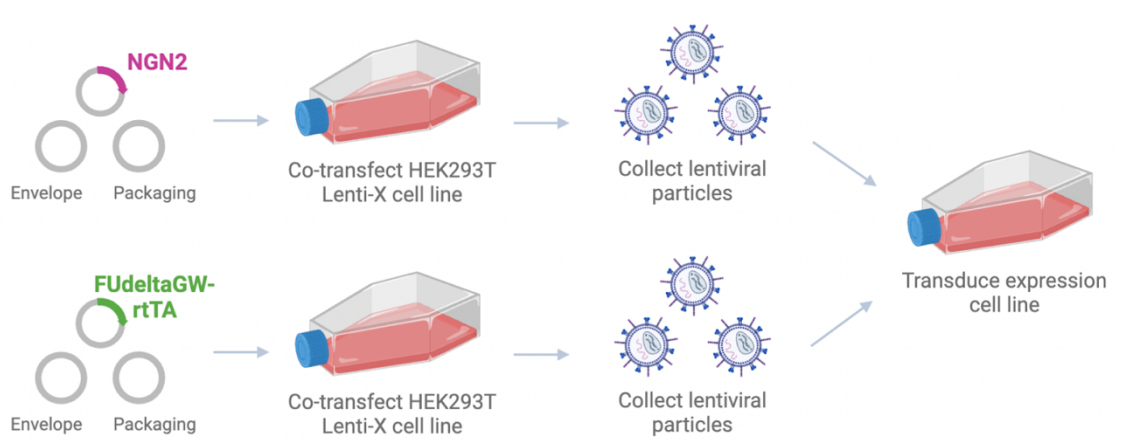

Figure 7. Workflow with the main steps followed to transfect SH-SY5Y cells with gene NGN2 and FUdeltaGW-rtTA using lentivirus. Generated with www.biorender.com.

During the lentiviral transfection of the NGN2 gene into SH-SY5Y cells, a specialized procedure is followed to introduce the NGN2 gene into the cells using a modified virus called lentivirus. To prepare the lentivirus, the NGN2 gene is incorporated into the viral genetic material in the laboratory. To produce lentivirus, HEK cells are cultured until they reach 40-50% confluence. Once achieved, the plasmids of interest (NGN2 and FUdeltaGW-rtTA), along with the packaging plasmids (pMD2.G and psPAX2), are transfected into the HEK cells using a commercial polycationic system (lipofectamine 3000).

The media produced by the transfected HEKs which contain the viral particles is collected and replaced by new media, repeating the process for 3 days. After this period, the supernatant is pooled together, filtered, and concentrated using Lenti-X concentrator.

Once the lentivirus carrying the NGN2 gene is ready, the SH-SY5Y cells are cultured and prepared for transfection. During the infection step, a solution containing Polybrene, and lentivirus is prepared and applied to the SH-SY5Y flask. The solution is added dropwise, and the cells are incubated overnight. The following morning, the medium must be changed to normal medium. For cell selection, after 48 hours a medium containing Puromycin is added. Non-transfected cells will die within 48-72 hours, allowing for the selection of successfully transfected cells.

Once the cells containing the construct of interest and the cells without it have been obtained, it is necessary to expand them and cryostore for the following experiment (for the complete protocol see Annex 2).

4.2.3. SH-SY5Y differentiation

This section involves differentiating SH-SY5Y into neuronal-like cells by combining a standard biochemical induction with using a novel genetically inducible system. The cell differentiation process used in this study is based on the protocol described by Dravid et al. (refer to Annex 4 for the precise protocol) with specific modifications such as replacing retinoic acid with EC23, or the

addition of doxycycline. The steps followed to induce neuron-like cell differentiation using the SH-SY5Y cell line, both with and without the NGN2 gene, are presented in Figure 8 [50].

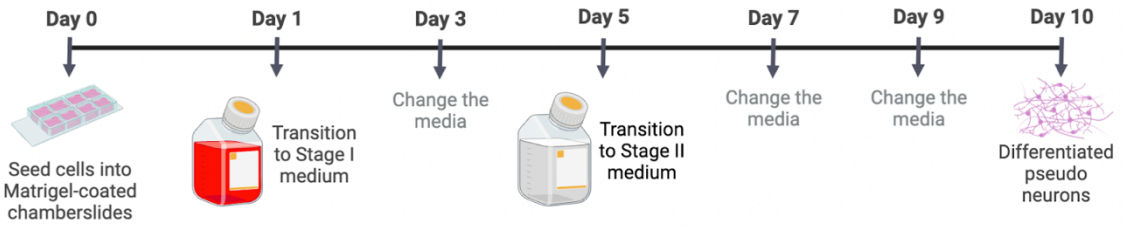

Figure 8. Process followed for differentiation of SH-SY5Y cells into neuronal-like cells. Generated with www.biorender.com.

The experimental procedure begins on day 0 by seeding 25,000 cells per well in two 8-chamber slides coated with Matrigel, utilizing a Neubauer chamber for cell counting. For comprehensive instructions on cell counting, please refer to Annex 1.5. Each cell type, with or without the construct, is arranged in separate rows within the slides. On the following day, the medium is replaced to introduce the Stage 1 medium. The Stage 1 medium is prepared by combining DMEM:F12 with iFBS (2.5%), 1x PS-L-Glut, and EC23 and doxycycline 2 µg/mL. On day 3, the medium is changed, and on day 5, the medium is further substituted with the Stage 2 medium. The Stage 2 medium consists of Neurobasal-A medium supplemented with BDNF (50 ng/mL), KCl (20 mM), B27 and PS-L-Glut. The medium is subsequently changed on days 7 and 9, with the culmination of the experiment occurring on day 10, at which point the cells are deemed to be fully differentiated. Moreover, laminin has been applied on days 3, 5 and 7 to help diminish the detachment of cells.

Table 4. Table including the reagents used of each medium, the stock concentration and the final concentration.

	REAGENT	[STOCK]	[FINAL]
STAGE 1 MEDIUM	DMEM:F12	-	-
	P/S-L-Glut	100x	1x
	iFBS	100%	2.5%
	EC23	10 mM	10 µM
	Doxycycline	10 mg/mL	2 µg/mL
STAGE 2 MEDIUM	Neurobasal medium	-	-
	B27	1x	50x
	BDNF	50 mg/mL	10 µg/mL
	P/S-L-Glut	1x	100x
	KCl	2 M	20 mM
	Laminin	1 mg/mL	1 µg/mL

4.2.4. Cell viability (PrestoBlue)

The subsequent step entails assessing the viability of cells at various concentrations of doxycycline to ascertain the optimal dosage for our experimental purposes. During the 2 media changes occurring along the first 5 days of differentiation, different concentrations of Doxycycline are applied to each column of the plate: 0.25, 0.5, 1, 2, 5, and 10 ug/ml. At day 5 of differentiation, 10 µL of

PrestoBlue is added to each well. Two controls will be used: three wells with medium (not cells) in which PrestoBlue will be added (Blank), and three wells with only medium as negative control. After 2 hours of incubation, the media is collected in a second plate and trespassed to another plate in the positioning shown in Figure 9 below. Cells get new media and continue the differentiation until the end.

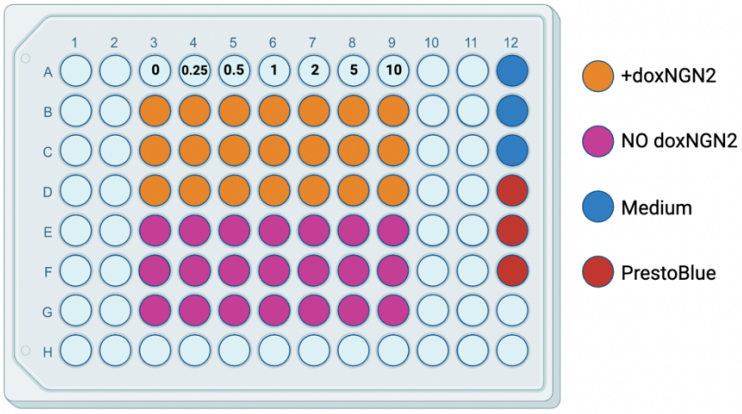

Figure 9. Scheme of final position of the solutions introduced in the 96-well plate. The A-row shows the concentrations of doxycycline applied on each column can be seen. Generated with www.biorender.com.

The readout of the fluorescence will be performed using an Infinite M200 PRO Multimode Microplate reader. The settings will be the ones suggested by the manufacturer, with an excitation wavelength of 560 nm and the emission wavelength of 590 nm. Then the machine will proceed to read the fluorescence of each individual well in the plate, capturing the data inside an Excel file for further analysis (for detailed guidance on the protocol for PrestoBlue usage, consult Annex 3).

4.2.5. Poly-acrylamide gel preparation

The fully differentiated cells will be seeded onto gels with 30 kPa and 1.5 kPa stiffness levels to investigate their mechanosensitivity. The subsequent steps detail the protocol for fabricating polyacrylamide gels on top of a glass surface with the specified stiffness values. However, for a comprehensive description, please refer to Annex 5.

The glass surface is prepared for gel deposition through silanization by applying a mixture of Acetic Acid and Bind Silane in ethanol 96% for 1 hour. Following incubation, the surface undergoes rinsing with Ethanol 96% and is left to completely air dry.

For the preparation of the gel mixture, a solution of PBS, 40% Acrylamide, and 2% BisAcrylamide is created according to the proportions to generate the desired stiffness (see Annex 5). After degassing, latex beads, APS, and TEMED are added to the solution to induce polymerization. Finally, a drop of 22 µL of the final solution is added to the glass, and an 18 mm glass coverslip is positioned on top. Polymerization of the mixture is allowed to occur over a period of one hour.

Subsequently, the gel-covered sample is immersed in PBS, and the coverslip is cautiously removed using tweezers.

The subsequent step entails the functionalization of the hydrogel by applying an ECM protein. The gels are then covered with a solution of sulfo-SANPAH and exposed to UV light for 7 min. The gels are subjected to washing steps employing HEPES and PBS solutions. Following the washing process, a solution of 20 ug/ml of laminin is added on the top of the gels, which are then incubated in the fridge overnight. The entire process can be seen in Figure 10.

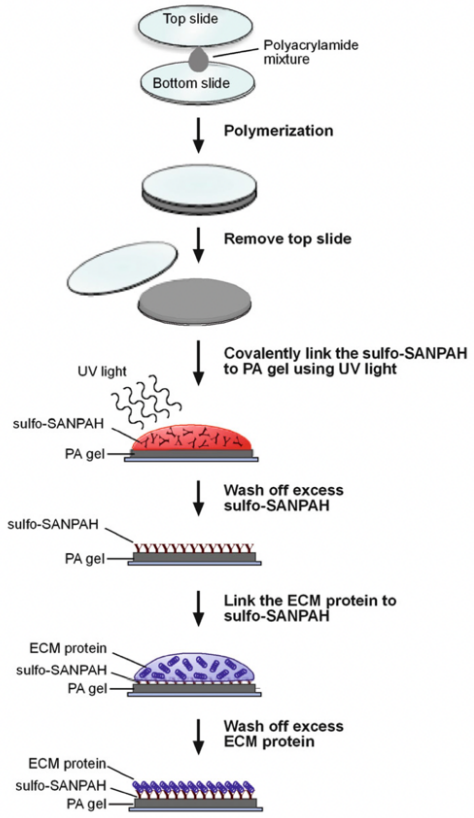

Figure 10. Schematic overview of the setup for making synthetic substrata. The gel-glass composite contains the amino-silanated coverglass (bottom slide), polymerizing acrylamide solution, and chloro-silanated coverglass (top slide). The polyacrylamide gel is functionalized by cross-linking sulfo-SANPAH at 365 nm followed by attachment of desired ECM protein. Extracted from Lee and Nelson (2013) [73].

The following morning the gels are washed, UV lighted for sterility purposes and placed inside the cell incubator covered in cell media. Neuronal-like cells are detached, counted, and seeded onto the laminin-coated polyacrylamide gels. 10.000 cells are added to each gel, to keep a low cell density compatible with single cell resolution analysis. Cells are allowed to attach and spread for 48h before fixation and posterior analysis.

4.2.6. Immunocytochemistry

Immunostainings targeting neuronal markers will be conducted to evaluate the maturity achieved during cell differentiation and assess the mechanosensitivity response of pseudo neurons. However, before initiating the immunocytochemical analyses, it is necessary to perform cell fixation.

The protocol involves washing the cells with warm PBS, fixing them with 4% paraformaldehyde for 12 minutes at room temperature, and then performing additional washes with PBS. In the case of handling delicate samples, a modified procedure is implemented to ensure their integrity. This involves preserving a portion of the volume during the wash step and introducing an additional wash cycle to prevent the cells from drying out.

Upon completion of the cell fixation process, the subsequent step involves the execution of immunocytochemistry. The samples are initially washed with PBS and then treated with a solution of 0.1% Triton X100 in PBS. Following this, they are incubated with a 2.5% BSA solution which acts as a blocking agent to prevent non-specific binding of antibodies and other reagents to the sample. Then, the primary antibody is added, covering the samples, and incubated for a specific duration. The antibodies used for each step are defined in Table 5:

Table 5. Summary of the antibodies used in the immunocytochemistry and the specific dilutions needed.

	ANTIBODY	DILUTION
PRIMARY ANTIBODIES	MAP2 (mouse)	x1:250
	ß3 tubulin (mouse)	x1:300
	SMI31	x1:250
	NGN2	x1:250
	YAP	x1:200
	TAU	x1:400
SECONDARY ANTIBODIES	Donkey anti-Ovine, Alexa Fluor™ 488	x1:500
	Goat anti-mouse, Alexa Flour™ 488 conjugated	x1:500
	Donkey anti-mouse, Alexa Fluor™ 555	x1:500
	Goat anti-Rabbit, Alexa Fluor™ 555	x1:500

After washing with PBS, the samples are incubated with the corresponding secondary antibodies and Hoechst 33342 DNA stain. Following another round of PBS washing, the samples can be mounted if required, using Mowiol. Finally, the samples are ready for imaging or can be stored at 4°C.

4.2.7. Confocal Microscopy

Image acquisition of fluorescent preparations was done with a Zeiss LSM880 inverted confocal microscope objective and using Zeiss ZEN 2.3 SP1 FP3 (black, version 14.0.24.201), Two kind of objectives were used: 20x Objective Plan-Apochromat (NA 0.8) for samples seeded on regular cultures plates, and a 40x immersion objective LD LCI Plan-Apochromat 40x (NA 1.2) (glycerol) for gels. The following combination of lasers was used: Diode 405-30 (405 nm, for Hoescht), Argon

(488 nm, for Alexa Fluor™ 488) and DPSS 561-10 (561 nm, for Alexa Fluor™ 555). Images were acquired at a resolution of 1024x1024 pixels, pixel dwelling 1.04 sec, averaging 2 (line). A graph of the excitation and emission spectra of the different fluorophores and the excitation lasers can be seen in Figure 11.

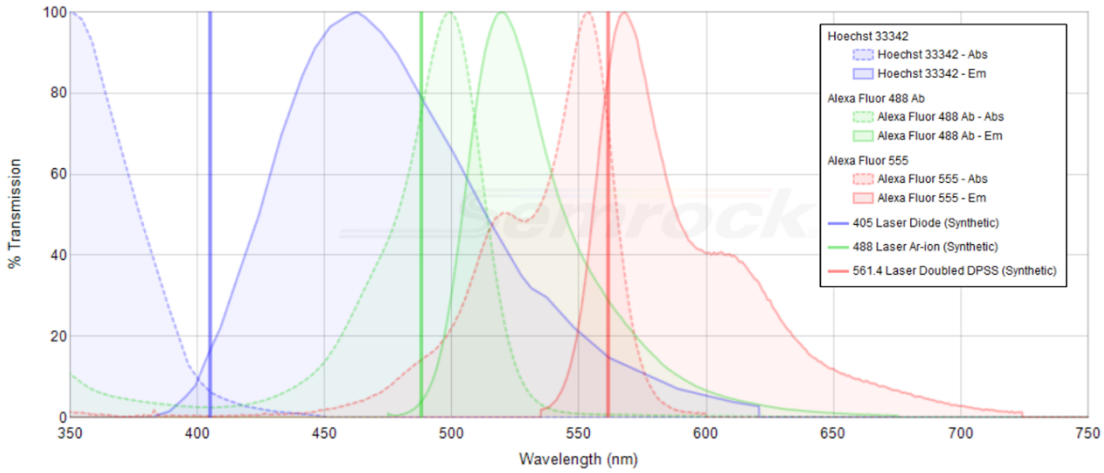

Figure 11. Graphical representation of the excitation and emission spectra of the fluorophores used in the immunofluorescence, as well as the Lasers used. The graph was made using SearchLight™ online tool.

4.2.8. Image Analysis

Image J was used to calculate through βIII-tubulin images the cellular morphology and circularity, a shape descriptor which indicates the degree of similarity to a perfect circle following this equation:

$$4\pi \cdot \frac{[Area]}{[Perimeter]}$$

A circularity value of 1.0 indicates a perfect circle, while a value closer to 0.0 indicates a shape that is progressively less circular.

Image analysis of YAP subcellular localization was performed using the Intensity Ratio Nuclei: Cytoplasm Tool (RRID: SCR_018573) ImageJ plugin. Single cell images taken for each stiffness were separated into nuclear channels (Hoesch) and signal channels (YAP). The following settings were used for correcting background: Radius = 1, Offset = 1, Iterations = 2, Skip limit = 0.05. For image analysis, Huang thresholding method was used. The validity of the analysis was assessed by visual control of the segmentation images produced by the plugin. The data is presented as the ICN factor, the factor between the cytoplasm and the nuclei intensity, equation is below.

$$ICN = \frac{\%\ intensity\ nuclei}{\%\ intensity\ cytoplasm}$$

4.2.9. Statistical analysis

All data were derived from three independent experiments and are represented as the mean ± s.d. Statistical analysis was performed with GraphPad Prism 8.0.0. For cell viability, statistical analyses were performed using Kruskal-Wallis test followed by post hoc multiple comparisons by Dunn's test. P>0.05 was not considered statistically significant. For shape descriptors and YAP nuclear: cytoplasmic ratio unpaired t-test was used. For single cell analysis, 30 cells from 3 different gels were analysed. All micrograph images shown in the figures are representative examples of results from the three different experiments.

5. DETAIL ENGINEERING

This section presents the comprehensive results obtained from the conducted experiments as described in the Concept Engineering section. The data collected and analysed provide valuable insights into the phenomenon under investigation. Moreover, the implications of these findings will be thoroughly discussed, shedding light on their significance and potential contributions to the existing body of knowledge in the field.

5.1. Cell viability results

As stated in the previous section, we firstly proceed to evaluate the effect of doxycycline treatment in cellular viability in order to rule out toxic effects after application during cell induction. For this assessment, Prestoblue was added to the SH-SY5Y treated with different concentrations of doxycycline at day 5 of differentiation. Both cells with and without the inducible NGN2 cassette were evaluated in triplicate. The change of colour from the oxidized form of resazurin (blue) to the reduced form (pink) was monitored visually every 30 minutes, until a noticeable change of colour could be observed at 2 hours (see Figure 12).

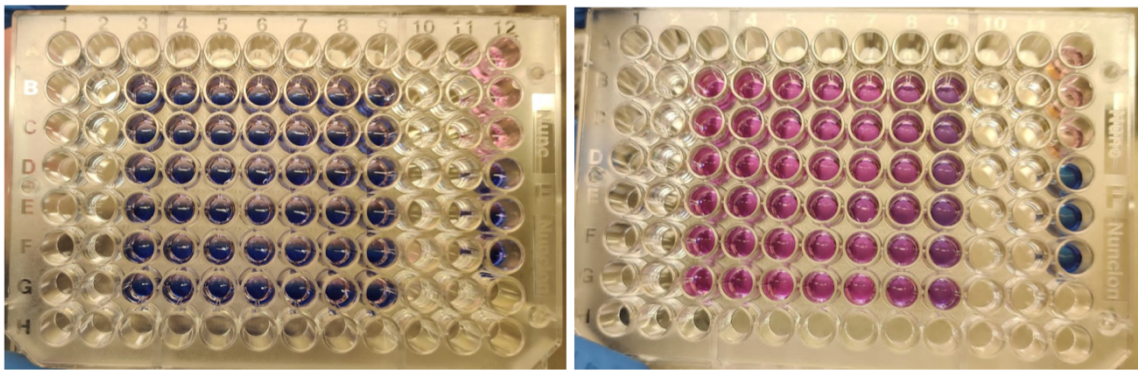

Figure 12. Colour shift of PrestoBlue solution in SH-SY5Y cells after 2 hours of incubation.

The results of the fluorescent readout are presented in Figure 13 below as the mean ± standard deviation (sd), with higher values indicating a higher cellular number in the well. No differences between the cell number of cells with the construct (blue, mean+sd) and without the construct

(yellow, mean+sd) was observed in the absence of doxycycline, indicating thus that the viral transduction per se does not affect cellular survival and/or proliferation. Moreover, no differences between both cell groups were detected at any of the concentration of doxycycline, confirming that the construct does not confer any resistance of detriment to the presence of the antibiotic.

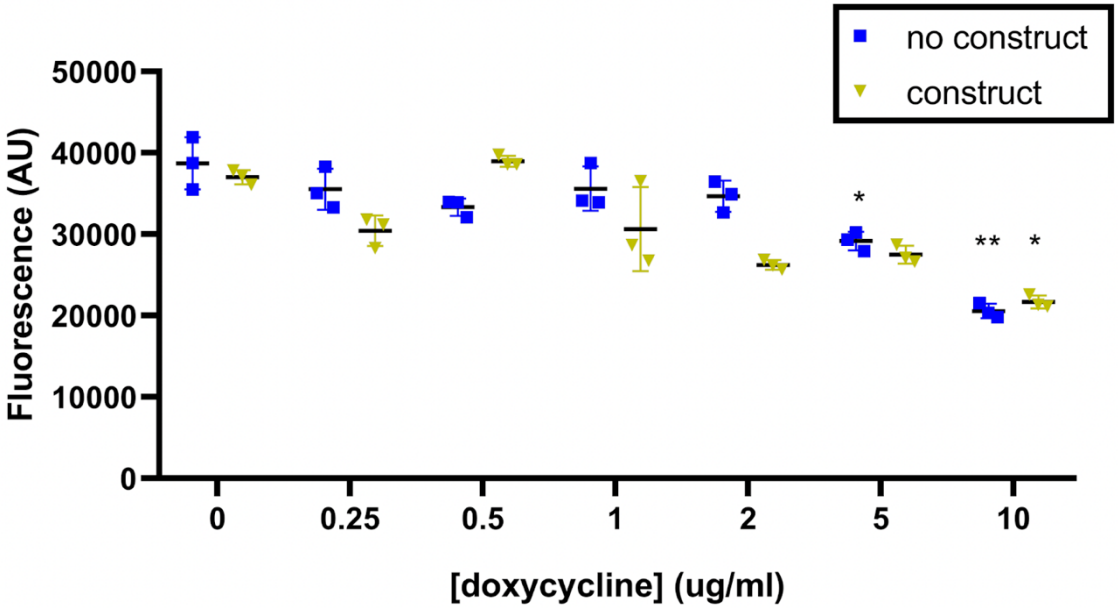

*Figure 13. PrestoBlue fluorescent intensity as a measure of the cell viability for each of the concentrations of doxycycline and cells containing the NGN2 inducible construct (yellow) or control (blue). Data represents mean±SD (n=3). * p-value > 0.05, ** p-value < 0.01 (Kruskal-Wallis test followed by post hoc multiple comparisons using Dunn's test).*

The comparison within the groups at different concentrations of doxycycline shows that no significant changes are observed in terms of the cellular viability until the doxycycline concentration reaches 5 µg/ml (for cells without the construct) and 10 µg/ml. This observation leads to the conclusion that concentrations exceeding 5 µg/ml exhibit cytotoxic effects on the cells.

Based on the aforementioned considerations, we concluded that the optimal doxycycline concentration for inducing neurogenin2 expression during differentiation is 2 µg/ml, ensuring a heightened response while mitigating cell death. Therefore, all the following experiments will be performed using that concentration.

5.2. Morphological assessment of SH-SY5Y differentiation

A preliminary assessment to evaluate the differences in neuron-like differentiation between cells with and without the induction of NGN2 expression was conducted by visual analysis of cellular morphology at different timepoints. Bright field images were acquired at key stages of the differentiation process (days 0, 5, and 10), as shown in Figure 14. The images reveal notable morphological differences in the commitment of SH-SY5Y cells towards neuronal fate with and without neurogenin2 expression at both timepoints.

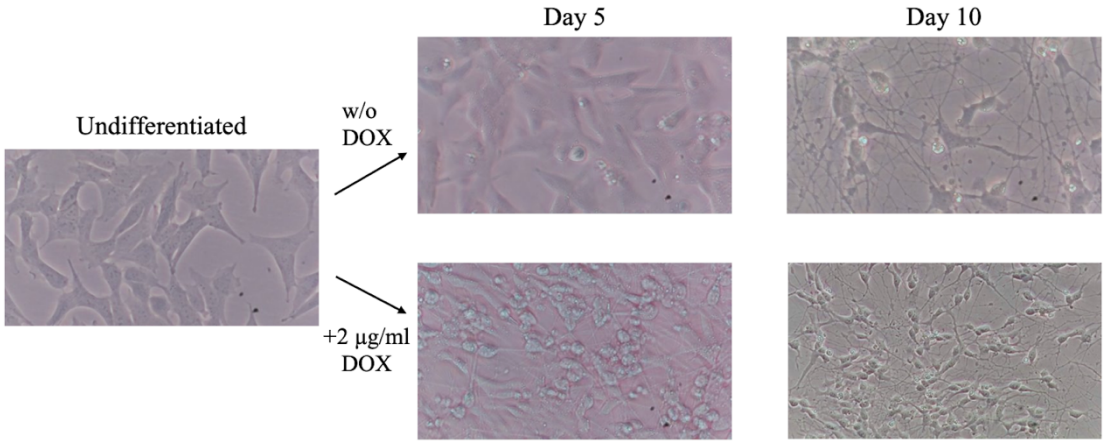

Figure 14. bright field images of SH-SY5Y cells with and without doxycycline at day 0, day 5 and day 10 of neuronal differentiation. Magnification used for the lens: 40x.

At day 5, cells having the induction of neurogenin2 by the addition of doxycycline exhibit smaller somas and begin to display neuronal terminations, suggesting a more advanced process of neuronal maturation in the presence of neurogenin2. On the contrary, cells without NGN2 induction display a morphology more similar to the undifferentiated cells, with a more spread cell body and still absent cellular protrusions. Furthermore, additional changes are observed in both cell groups at day 10. Cells with the neurogenin2 construct display a homogeneous population of neuron-like cells, with more rounded soma with a dense network of dendrites connecting them. In contrast, although cells without the construct showed evident morphological changes denoting neuronal commitment, they still exhibit more irregular shapes and higher cells spreading compared to the others. These morphological changes are a visual validation of the influence of neurogenin2 in neuronal differentiation.

5.3. Analysis of neuronal markers expression in SH-SY5Y cells

Following the visual examination along the differentiation process, cells were fixed at day 10 and stained for different markers of neuronal commitment by immunocytochemistry. Two proteins were stained in each preparation in order to maximize the amount of information obtained for each of them. By employing this method, we aimed to elucidate the differential protein expression profiles of relevant neuronal markers between the groups, the homogeneity of positivity between the cells and the subcellular distribution.

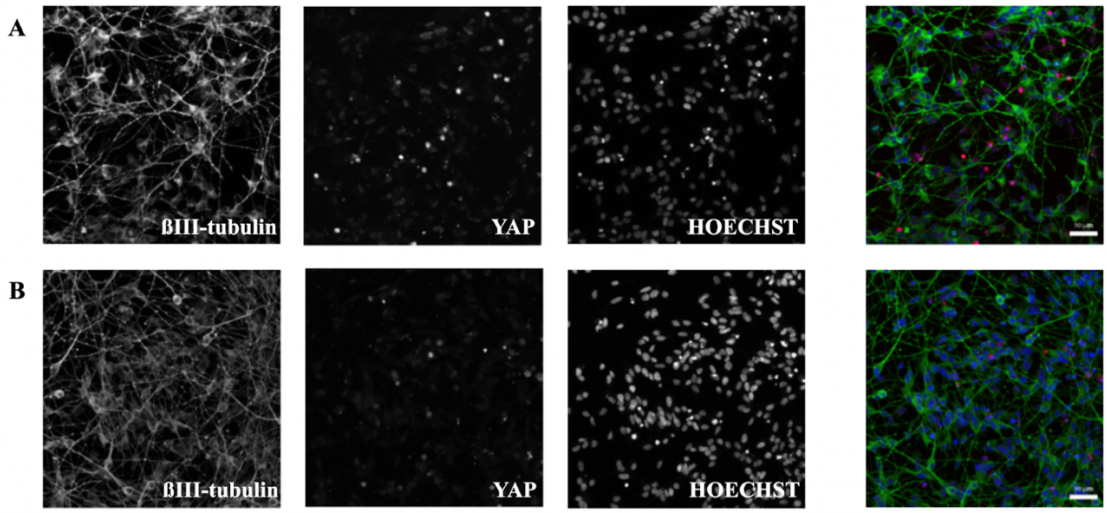

Figure 15. Confocal image of ßIII-tubulin and YAP immunostaining for neuron-like cells at day 10 without (A) or with (B) doxNGN2 construct. Cell nuclei were co-stained with Hoechst. The coloured image corresponds to the sum of all channels (green: ßIII-tubulin, red: YAP, blue: Hoechst). Scale: 50 µm.

Firstly, we investigated the expression of the most employed neuronal marker, ßIII-tubulin, in conjunction with the mechanoregulated co-transcription factor YAP.

Most of the cells in the preparations are positive for the pan-neuronal cytoskeletal protein ßIII-tubulin, which, as observed in the images, is incorporated into the microtubule network along the whole cell in both conditions. The images also confirm that the neuron-like cells have detectable levels of YAP, which will make it possible to determine its mechanoregulation. Under standard culture conditions, which correspond to a highly stiff environment, the distribution of YAP appears predominantly nuclear. Interestingly, the induction of neurogenin2 does not seem to induce any notable changes in YAP expression, contrary to the results of previous articles, which stated a possible “inhibition of YAP by neuronal-differentiation-inducing GPCR agonists such as PACAP or proneural genes (e.g., Ascl1 or Neurogenin2)." (Michu, 2013) [74].

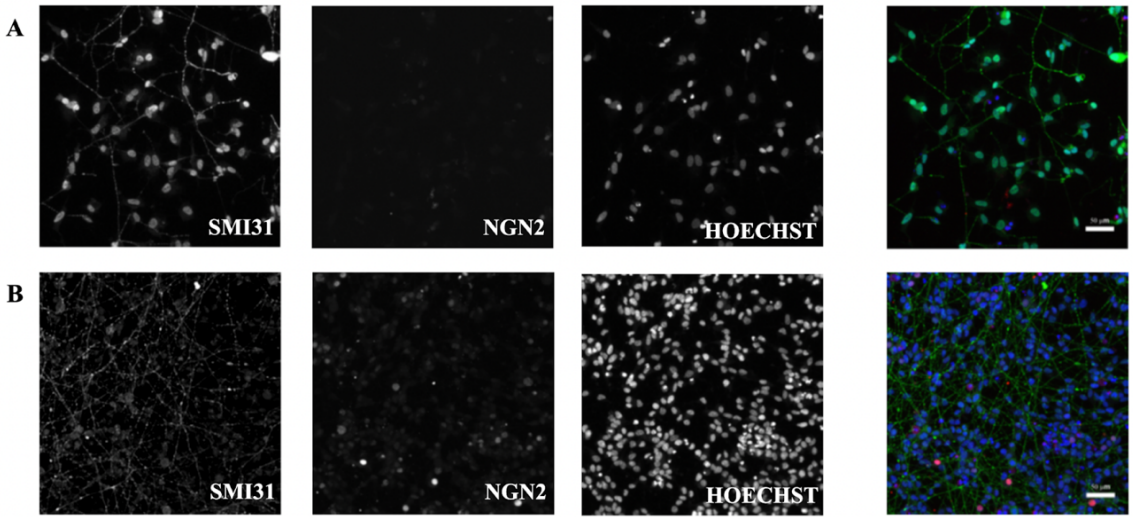

Figure 16. Confocal image of SMI31 and NGN2 immunostaining for neuron-like cells at day 10 without (A) or with (B) doxNGN2 construct. Cell nuclei were co-stained with Hoechst. The coloured image corresponds to the sum of all channels (green: SMI31, red: NGN2, blue: Hoechst). Scale: 50 µm.

In a parallel preparation, the distribution of two additional proteins were studied (Figure 16). The SMI31 antibody is a monoclonal antibody raised against neurofilament proteins H [75], which are predominantly localized in neuronal axons. However, subsequent experiments revealed that in the absence of phosphorylated neurofilament-H (NF-H), the antibody can recognize other phosphorylated forms of intermediate filaments, including phosphorylated lamin, a component of the nucleoskeleton [76]. This explains the staining pattern observed in cells without the construct, as the absence of phosphorylated NF-H allows the antibody to bind to the nucleus. Therefore, it can be inferred that increased phosphorylated NF-H levels in axons of cells with doxNGN2 correlate with enhanced maturation.

Additionally, higher levels of neurogenin2 expression are observed in cells with the construct, as they possess the integrated gene and are activated by doxycycline. However, basal expression of NGN2 is also detected in cells without the construct, suggesting that these cells endogenously produced neurogenin2 during differentiation to acquire neuronal characteristics. Consequently, this result validates that the overexpression of NGN2 is a physiologically relevant way to reinforce the neuronal commitment of the SH-SY5Y.

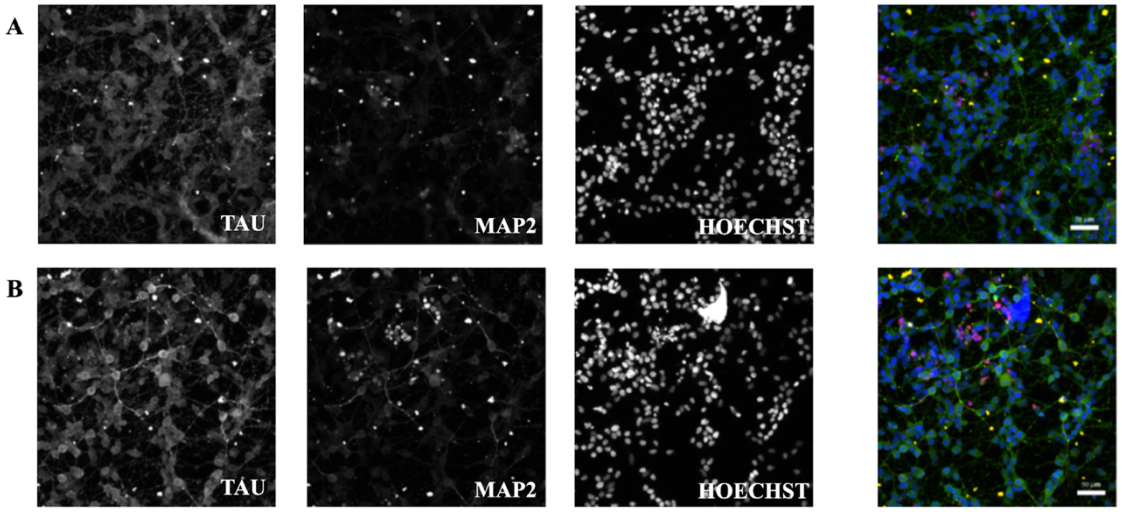

Figure 17. Confocal image of TAU and MAP2 immunostaining for neuron-like cells at day 10 without (A) or with (B) doxNGN2 construct. Cell nuclei were co-stained with Hoechst. The coloured image corresponds to the sum of all channels (green: TAU, red: MAP2, blue: Hoechst). Scale: 50 µm

In Figure 17, the focus of investigation shifts to the analysis of two proteins which are indicators of neuronal polarity, and therefore, cellular maturity: MAP2 and TAU. In mature neurons, a characteristic distribution pattern is anticipated, wherein MAP2 is confined to the soma and dendrites [77], while tau protein is primarily localized in the axon. As noticeable in the images both the cells with the construct and without the construct exhibit a relatively comparable expression of tau protein and MAP2.

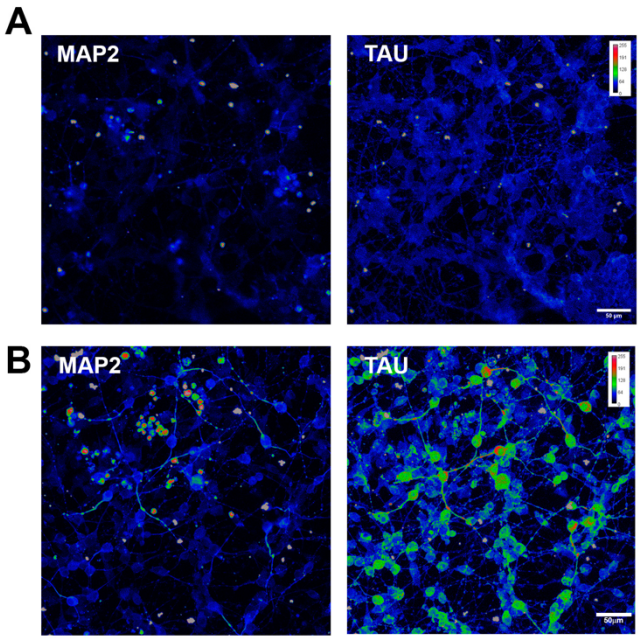

Figure 18. Rainbow RGB-colour coded intensity for the immunostaining images of TAU and MAP2 of neuron-like cells without (A) or with (B) doxNGN2 construct. Scale: 50 µm.

As it can be observed in the color-coded intensity image in Figure 18, cells with NGN2 induction showed higher intensity levels of TAU immunostaining. However, no clear intracellular compartmentalization is observed for any of the cytoskeletal proteins stained, i.e., similar intensity can be observed in the axons and soma.

Overall, the findings from our study provide compelling evidence that the overexpression of NGN2 exerts a significant influence on enhancing the neuronal commitment of SH-SY5Y cells. The experimental results demonstrate that NGN2 plays a crucial role in driving the cellular differentiation process towards a neuronal fate.

However, it is important to acknowledge that, despite the positive effects of NGN2 overexpression on neuronal commitment, our experiments revealed that the cells did not fully acquire a complete compartmentalization between the soma and axon during the specific timeframe of differentiation that was investigated. This observation implies that, although NGN2 promotes the initial stages of neuronal differentiation, additional factors or extended culture conditions may be required to achieve a more mature and functionally distinct neuronal phenotype.

5.4. Mechanoresponse of SH-SY5Y neuron-like cells to matrix stiffness

5.4.1. Morphological analysis of SH-SY5Y neuron-like cells in the hydrogels

Once confirmed that cells with NGN2 induction have a higher degree of differentiation and they express detectable levels of YAP protein, we proceeded to investigate their response to substrate stiffness. The morphology of several cell types has been shown to be influenced by the stiffness of the ECM. When cultured in vitro, cells placed on soft, two-dimensional ECM substrates tend to

exhibit a relatively small and round shape, whereas on stiffer ECMs, cells adopt elongated shapes. In the case of highly rigid substrates like glass, cells tend to spread out and become flattened.

The neuron-like SH-SY5Y cells expressing the NGN2 construct were differentiated in regular tissue culture polystyrene and then reseeded in polyacrylamide gels with stiffness values of 30 kPa and 1.5 kPa, in which most of the cells tested in the lab showed different mechanoresponse.

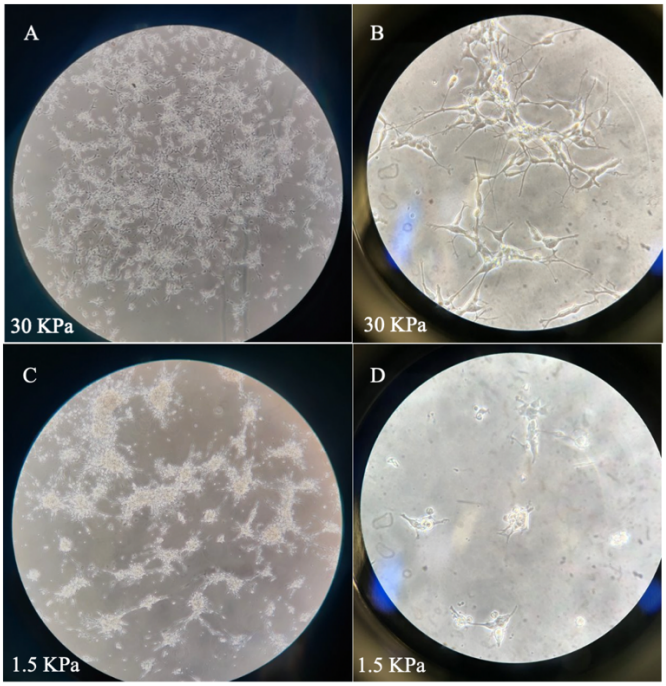

Figure 19. Bright field images of SH-SY5Y neuron-like cells seeded onto PA gels with different stiffnesses. Cells onto the 30 kPa gel at a magnification of 10x (A) and 40x (B). Cells onto the 1.5 kPa gel at a magnification of 10x (C) and 40x (D).

As shown in Figure 19, at simple visual examination neuron-like cells exhibit greater spreading on substrates with higher stiffness, while at 1.5 kPa they tend to form cellular colonies or aggregates. At a higher magnification of 40x, the morphological differences o of the pseudo neurons are highlighted, with cells exposed to higher substrate stiffness displaying more elongations and to mature neurons.

To further validate the morphological changes, cells were stained for ßIII-tubulin, a marker distributed along the whole cell body (Figure 20). Single cell analysis confirmed that neuron-like cells showed a significantly higher spreading area at 30 kPa (167.3 ± 76.13 μm^2) in comparison to 1.5 kPa (63.9 ± 24.20 μm^2). Moreover, the calculation of circularity index also demonstrated that cells in the softer substrates showed a projected area closer to a circle (0.7055 ± 0.1418) than the ones in stiffer gels (0.3517 ± 0.1284). Therefore, these changes in cellular morphology confirm that neuron-like cells are able to sense the substrate stiffness.

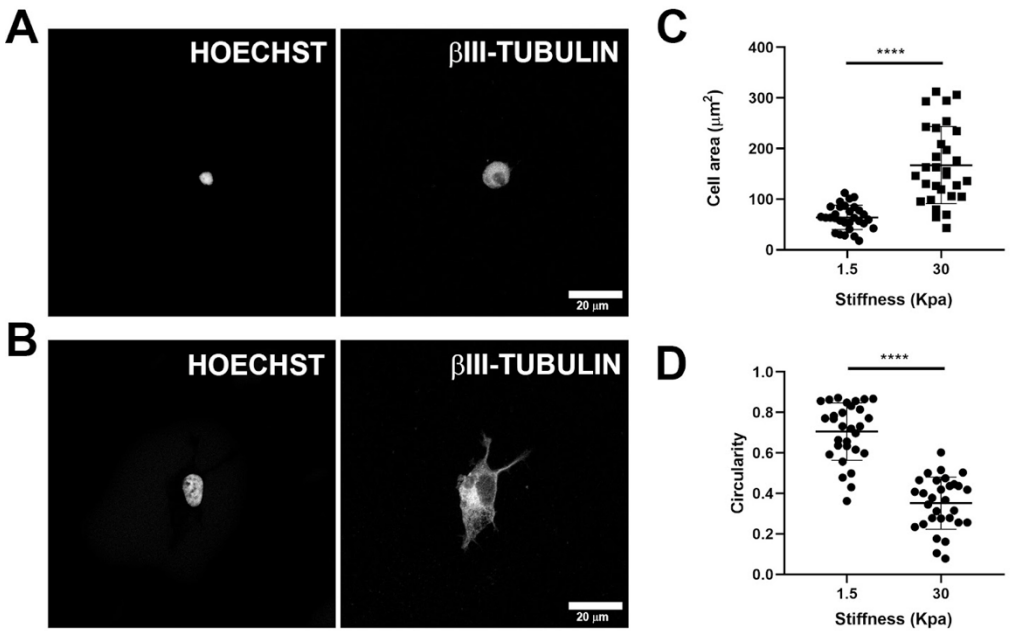

*Figure 20. Image analysis of the neuron-like cells seeded onto polyacrylamide gels. Immunostaining for ßIII-tubulin and Hoechst for cells in 1.5 kPa (A) and 30 kPa (B). Scale bars: 20 µm. ßIII-tubulin were used to calculate the projected cell area (C) and Circularity index (D). ****P-value<0.0001.*

5.4.2. Mechanoregulation of YAP nuclear localization

As a final step of the project, the sensitivity of the nuclear localization of YAP to matrix stiffness was analyzed through immunostaining. As explained before, when most of the cells are cultured on a soft matrix or in low-stiffness conditions, YAP tends to be predominantly localized in the nucleus. In contrast, on a stiff matrix or in high-stiffness conditions, YAP is often sequestered in the cytoplasm. While in our previous experiment and previous literature YAP has been found present in neurons, its mechanoregulation has not been proved yet. Therefore, the cells were stained for YAP and ßIII-tubulin, and using an image analysis tool, the Index Cytoplasm: nucleus (ICN) for cells in both of the stiffness was calculated (Figure 21). As predicted, cells in the soft gel presented a low YAP ICN factor (0.7364 ± 0.43049), indicating that in this condition YAP is mostly found in the cytoplasm. On the contrary, cells exposed to high stiffness displayed a distinctive nuclear pattern for YAP staining, which corresponded to a significantly higher ICN (1.554 ± 0.8037).

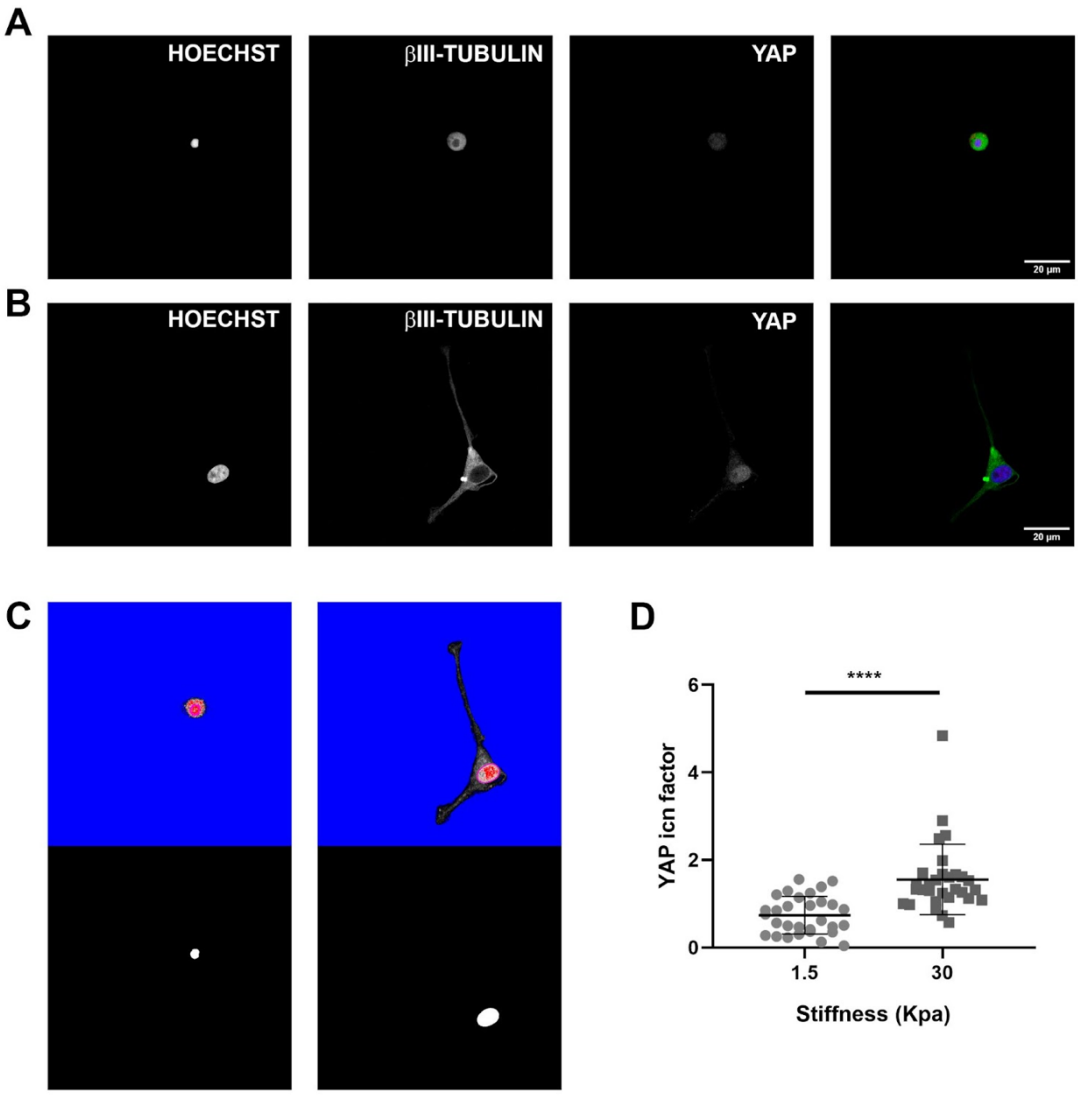

*Figure 21. Confocal image of ßIII-tubulin and YAP immunostaining for neuron-like cells seeded on 1.5 kPa (A) or 30 kPa (B) gels. Cell nuclei were co-stained with Hoechst. The coloured image corresponds to the sum of all channels (green: ßIII-tubulin, red: YAP, blue: Hoechst). C. Example of YAP nuclear-cytoplasmic analysis by the ImageJ plugin for neuron-like cells growing in soft (left) and stiff (right) hydrogels. D. YAP ICN factor for both stiffness studied. ****p-value<0.0001. Scale: 20 µm.*

In conjunction, our results demonstrate that SH-SY5Y-derived neurons are mechanosensitive to matrix stiffness and have the proper mechanisms to regulate the nuclear localization of YAP in response to the ECM rigidity in which they are growing.

6. EXECUTION SCHEDULE

To provide a methodical and organized approach, a detailed description of the WBS of the project is presented in this blog of the report. Through this tool, the individual activities that comprise the work plan are identified and detailed in the WBS dictionary. In addition, two diagrams have been developed to visually illustrate the flow of activities and the possible flexibility in delivery dates. This rigorous and structured approach ensures proper project management and maximizes the likelihood of successful project execution.

6.1. Work Breakdown Structure

The detailed work breakdown structure shown in Figure 22 has been developed. It identifies the different tasks that make up the project and are necessary for its success.

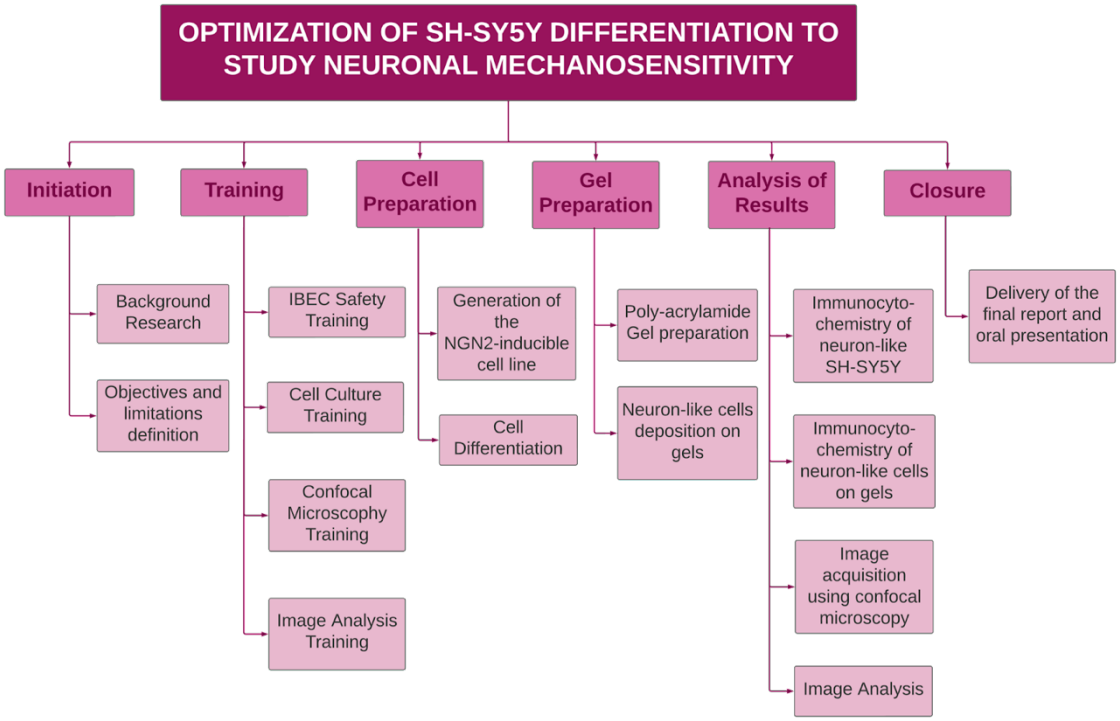

Figure 22. WBS scheme of the project. Generated with https://lucidspark.com.

The activities are divided into different levels in a hierarchical way, achieving maximum specificity and dividing the execution process into different phases. This work structure is of great help in subsequently defining an optimal budget and establishing a feasible schedule. First, there is the final product: the project. Then, there are six main divisions corresponding to the second level work blocks: Concept Engineering, Design Plan, Resourcing and Delivery. Finally, these four groups are broken down into different, more concrete tasks that form the basis of the project. For example, the first work package includes Documentation and Definition of Objectives, two essential tasks to establish the direction the idea will take.

6.1.1. WBS Dictionary

The WBS dictionary is presented below and is used to show in detail all the activities that have been previously defined in the scheme of work. This dictionary is presented in table format and includes all the important aspects of each work package that has been defined.

Table 6. WBS dictionary of the "Initiation" work package.

INITIATION

Nº	Name	Duration	Description
1.1	Background research	7 days	Consists on searching for information on the state of technology, background, and ultimately conducting a complete market analysis in order to optimally shape the objectives, design, and methodology of the project.
1.2	Objectives and limitations definition	7 days	Specify the goals of the project to consider it successful, the purpose and how to achieve it, as well as the characteristics it must have. It is necessary to specify and be aware of the limitations of the study.

Table 7. WBS dictionary of the "Training" work package.

TRAINING

Nº	Name	Duration	Description
2.1	IBEC safety training	7 days	Program to ensure a safe and secure working environment for its researchers, staff, and visitors. Learn about potential hazards associated with working in a bioengineering laboratory and to mitigate risks and prevent accidents.
2.2	Cell culture training	7 days	Achieving the necessary knowledge to perform cell culture effectively and safely in a laboratory environment. The key aspects include the proper handling of culture hoods, cell transfer and fixation techniques, preparation and creation of culture media, as well as where to find the materials to be used.
2.3	Confocal microscopy training	4 days	Learn how to operate the confocal microscope, familiarizing oneself with its key components and functions.
2.4	Image analysis training	3 days	Get the necessary skills to use ImageJ's functions and tools, including image loading, adjustments, measurements, filters, etc.

Table 8. WBS dictionary of the "Cell preparation" work package.

CELL PREPARATION

Nº	Name	Duration	Description
3.1	Generation of the NGN2-inducible cell line	10 days	Introduction of the NGN2 gene into SH-SY5Y cells using an appropriate viral vector with the aim that the cells begin to express and produce the NGN2 protein.
3.2	Cell differentiation	28 days	Perform differentiation of SH-SY5Y cells into neuron-like cells.

Table 9. WBS dictionary of the "Gel preparation" work package.

GEL PREPARATION

Nº	Name	Duration	Description
4.1	Poly-acrylamide gel preparation	2 days	Fabrication of gels with customized stiffness (30 kPa and 1.5 kPa) by following a standardized protocol.
4.2	Neuron-like cells deposition on gels	2 days	The deposition process entails carefully placing or applying these cells onto gel substrates with specific stiffness, allowing them to adhere and interact with the gel material.

Table 10. WBS dictionary of the "Analysis of results" work package.

ANALYSIS OF RESULTS

Nº	Name	Duration	Description
5.1	Immunocytochemistry of neuron-like SH-SY5Y	7 days	Perform an immunocytochemistry of differentiated SH-SY5Y cells with and without construct to study the expression of specific proteins.
5.2	Immunocytochemistry of neuron-like cells on gels	7 days	Perform an immunocytochemistry of differentiated SH-SY5Y cells on top of gels with different stiffnesses to evaluate the response to mechanical stimuli.
5.3	Image acquisition using confocal microscopy	14 days	Obtain images of both immunohistochemistry applied using a confocal microscope.
5.4	Image analysis	14 days	Perform image analysis of the images obtained during 5.3 to derive project conclusions and assess the initial hypotheses.

Table 11. WBS dictionary of the "Closure" work package.

CLOSURE

Nº	Name	Duration	Description
6.1	Delivery of the final report and oral presentation	14 days	Delivery of the written work that has been developed throughout the project's progress and preparation and execution of an oral presentation summarizing the main steps and findings of the project.

6.2. PERT Diagram

The Program Evaluation and Review Technique (PERT) diagram is a tool employed for the detailed scheduling, planning, and organization of project tasks. As previously identified, the activities have been listed, and the subsequent step involves determining their interdependencies. By additionally calculating the duration in days of each activity, we obtain the matrix presented in Table 12, which will be utilized to construct the diagram.

Table 12. Precedence and time matrix for calculating the PERT diagram.

ID	Name	Predecessor	Duration in days
0	Background research	-	7
1	Objectives and limitations definition	0	7
2	IBEC safety training	1	7
3	Cell culture training	2	7
4	Confocal microscopy training	10,11	4
5	Image analysis training	12	3
6	Generation of the NGN2-inducible cell line	3	10
7	Cell differentiation	6	28
8	Poly-acrylamide gel preparation	7	2
9	Neuron-like cells deposition on gels	8	2
10	Immunocytochemistry of neuron-like SH-SY5Y	7	7
11	Immunocytochemistry of neuron-like cells on gels	9	7
12	Image acquisition using confocal microscopy	4	14
13	Image analysis	5	14
14	Delivery and oral presentation	13	14

Figure 23 depicts the sequential arrangement of tasks, where the critical path is characterized by the activities highlighted in red, denoting a 5-day margin for activity 10. The sequential structure of the PERT diagram in a research paper project can be attributed to the logical progression of interdependent tasks inherent in the research process. Each task is contingent upon the completion of its preceding task, establishing a linear dependency and sequential flow. For example, before conducting confocal microscopy for image acquisition, immunocytochemistry must be performed to prepare the samples. This emphasizes the necessity of following a pre-established plan where activities are initiated after the completion of preceding ones.

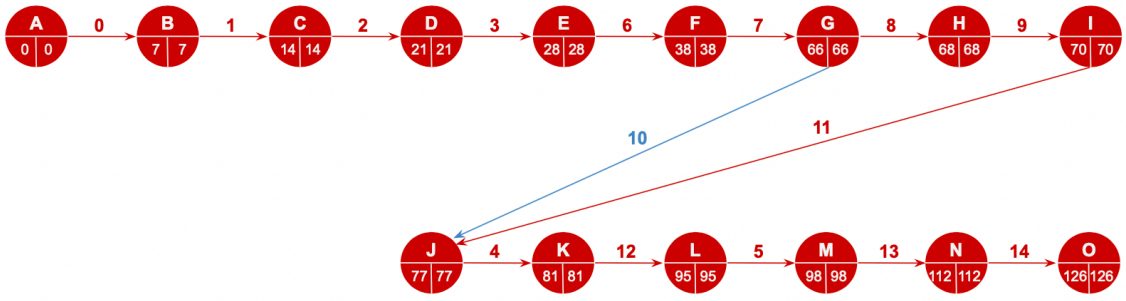

Figure 23. PERT diagram.

6.3. GANTT Diagram

The following tool is also used for project planning, providing an overview of tasks along with their start and end dates. The Gantt chart depicted in Figure 24 shows that the x-axis represents the activities defined in the WBS, while the y-axis represents the project timeline in days. The chart spans a total duration of 126 days or 4.5 months, from February to the middle of June. Task durations are indicated in two different colours, with violet indicating tasks that have some flexibility and red indicating tasks with no flexibility.

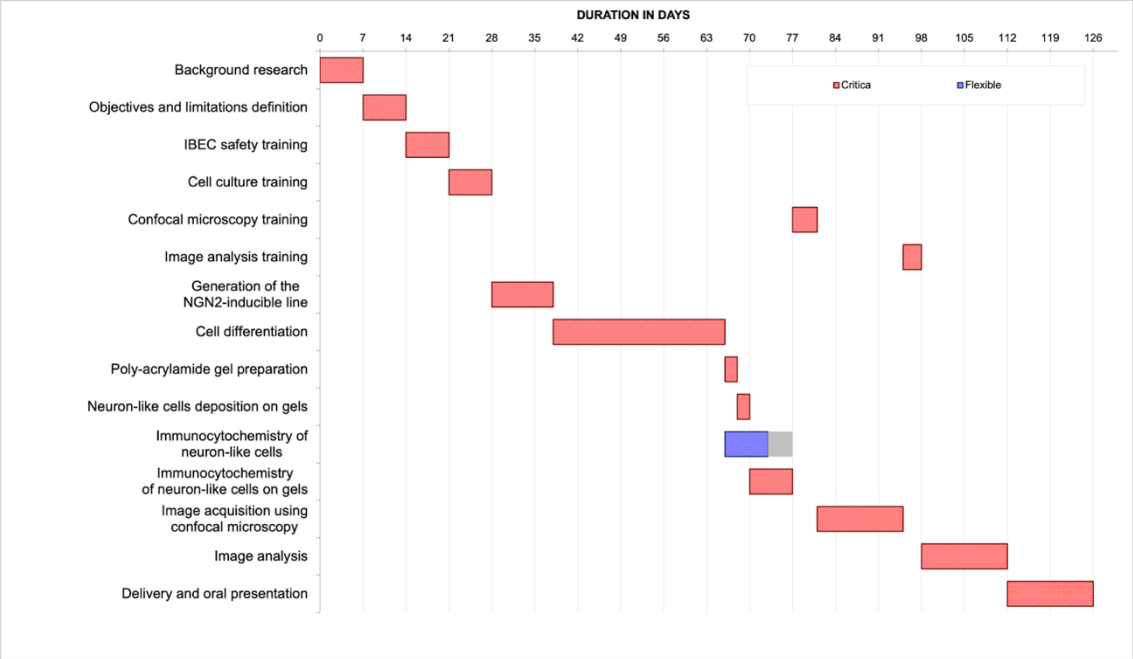

Figure 24. GANTT diagram.

The project exhibits a predominantly sequential progression, with experiments depending on the completion of previous ones. Therefore, careful consideration and mitigation of unforeseen events are crucial to avoid potential delays. To address this, a contingency margin has been incorporated into each activity, providing flexibility to accommodate any inconveniences.

7. TECHNICAL VIABILITY

A SWOT analysis is undertaken to explore the internal factors (strengths and weaknesses) and external factors (opportunities and threats) influencing the project in question. The internal factors represent the available resources, team qualifications, prior experience in similar projects, adaptability to change, etc. The external factors, on the other hand, assess the market conditions, existing competition, regulatory requirements, and the quality of the project team. The result obtained is shown in Table 13 and once studied, measures must be taken to address the challenges and take advantage of the opportunities identified to ensure the success of the project.

Table 13. SWOT analysis of the project.

Strengths	Weaknesses
Advanced technological resources and laboratory tools. Previous experience in performing similar research tasks. Availability of funding to support the research. High novel topic.	Time constraints to complete all tasks. Dependence on external resources such as samples or materials. Lack of previous knowledge in literature in which to base the research.
Opportunities	**Threats**
Growing interest in the study of cellular mechanisms, especially in Alzheimer's disease. Possible collaboration with other institutions or researchers. Access to databases and updated scientific literature. Participation in conferences and symposia to disseminate the results of the project.	Requires high skill and experience on the part of the team. Complexity and sensitivity of the techniques used. Changes in funding priorities that may affect the availability of resources.

Strengths

The present research project has diverse strengths which support its feasibility and contribute to its potential success. Firstly, advanced technological resources and laboratory tools are available, providing a robust and up-to-date infrastructure. In addition, the research group has funding to support the development of the experimental plan delineated and significant previous experience in carrying out similar scientific projects, which ensures an informed approach and a sound knowledge of the methods and techniques to be employed. Finally, the relevance of the selected research topic lies in its innovative and underexplored status, which allows for the possibility of original and significant contributions to the field of study.

Weaknesses

Despite the aforementioned strengths, this project also faces certain weaknesses that are important to be aware of and address appropriately. One highlighted weakness is the time constraint imposed by the framework, which may create additional pressure to complete all stages and activities within the established timeframe. The dependence on external resources, such as chemicals or specific materials, is also recognised, which introduces uncertainty and may lead to delays in obtaining them. In addition, a potential limitation in terms of specific expertise and knowledge is identified, especially regarding the application of particularly complex or novel experimental techniques or protocols, which may require an additional learning curve and the need for careful supervision by the research director. It is essential to address these weaknesses by proper planning, seeking expert advice and allocating additional resources if necessary.

Opportunities

The research project identifies several opportunities. Firstly, there is a growing interest in the study of cellular mechanisms, especially in relation to diseases such as Alzheimer's disease. This

suggests that there is a favourable context for research and the potential to generate significant impact in the field. Access to databases and updated scientific literature thanks to the University of Barcelona and IBEC is also highlighted, which provides a solid base to support the theoretical framework and allows for a thorough review of the existing literature. Finally, participation in conferences and meetings is mentioned, which provides a platform for dissemination of project results and interaction with other professionals and researchers in the field.

Threats

The research project also faces certain threats. Firstly, the need for the support of a highly trained and experienced team to address the technical and methodological challenges presented by the project is recognised. The complexity and sensitivity of the techniques used require in-depth knowledge and specialized skills to ensure reliable and accurate results. In addition, the potential for difficulties inherent in the techniques employed is identified, which may affect the quality of the data and results obtained. It also considers the possibility of changes in funding priorities, which could limit the availability of financial resources and affect the proper implementation of the project.

Furthermore, since the project is conducted in a research laboratory environment and given the highly specialized and sensitive nature of the techniques and protocols used in this context, it is essential to address and resolve more specific technical issues that may compromise the quality and integrity of the data obtained. A thorough assessment of the technical difficulties encountered is therefore necessary to ensure the feasibility of the project and the validity of its results.

Sterile cultures

Handling cells in a sterile environment is crucial to avoid contamination and maintain experimental integrity. Contamination by bacteria, fungi or even other cell types can lead to altered results and loss of time, resources and cells. Maintaining a sterile environment requires a thorough knowledge of sterilization techniques and working in a culture room that meets the required purity requirements. In addition, sterile equipment and materials must be available, including gloves, pipettes, culture media, incubators, and ovens, among others. Even with all precautions, contamination can still occur due to small human errors or equipment or material failures. Therefore, the measures adopted are adequate training, the routinary monitoring of mycoplasma contamination and visual observation of cellular finesses during culture, and an initial handling of the cultures under the supervision of the director.

Polyacrylamide gels

The creation of polyacrylamide gels is a time consuming and challenging technical task, with several steps that are critical for the final results. The preparation of the acrylamide solution demands precise measurements of the constituents, as even small variations in chemical concentration can significantly affect the consistency and quality of the final product, in terms of stiffness and homogeneity. In addition, the final release of the gel from the molding coverslip is a very delicate process that relies on care and precision to avoid damaging the gel. The seeding of

the neuronal-like cells on the gel is a complex process. Finally, the fixation and staining also require careful handling. Overall, both cell culture and gel preparation must be tightly coordinated in time, as a failure in one of them can result in the loss of almost 2 weeks of work.

Overall, the SWOT analysis gives us a complete picture of the internal and external factors that influence the research project while the detection of specific technical difficulties prevents future issues. By understanding and considering these aspects, we can make informed decisions, implement appropriate strategies, and maximize opportunities to make the study a success. Awareness of our strengths and weaknesses, along with the ability to take advantage of opportunities and mitigate threats, enables us to effectively move towards our goals and contribute to knowledge in our field of study.

8. ECONOMIC VIABILITY

The economic viability of a project relies on the balance between benefits and costs, ensuring efficient allocation of resources. In the context of this project, the final objective is to contribute with new knowledge, therefore direct benefits upon completion are not anticipated. However, it does yield indirect economic advantages through knowledge dissemination, including attracting future research funding, fostering industry collaborations, driving innovation, and enabling potential commercialization opportunities.

To comprehensively study the project's resource requirements, this section analyses the material, equipment, and human resources involved. The accompanying Table 14 provides a detailed breakdown of expenses, encompassing laboratory reagents for experiments, essential disposable materials like gloves and pipettes, and equipment costs factoring in lifespan and hours of use. Additionally, human resource costs encompass the student's work hours and the director's hours dedicated to supervision and training, valued at €8 and €20 per hour, respectively.

Table 14. Detailed costs of the project.

ITEM	QUANTITY USED	FINAL PRICE (€)
Reagents		
DMSO (Invitrogen™, D12345)	1 mL	3.87
70% ethanol (Sigma-Aldrich™, 470198)	2 L	191.75
DMEM/F12 (Gibco™, 11320033)	1 L	68.8
Fetal Bovine Serum heat inactivated (Gibco™, 10082147)	112 mL	155.46
Pen/Strep*L-Glut (Invitrogen™, 10378016)	100 mL	42.17
PBS (Gibco™, 10010002)	2 L	72.8
TrypLE Express™ (Gibco™, 12604013)	15 mL	3.08
Trypan Blue (Gibco™, 15250061)	0,1 mL	0.04

Plasmid NGN2 (Addgene, 34999)	5000 ng	85 $
pMD2.G (Addgene, 12259)	1750 ng	85 $
psPAX2 (Addgene, 12260)	3250 ng	85 $
HEK 293T cells (CLS, 300189)	1x	375
Lipofectamine 3000/P3000 reagent (Invitrogen™, L3000015)	50 µL	39.6
OptiMEM (Gibco™, 11058021)	1 mL	0.1
DMEM High glucose (Gibco™, 10569010)	500 µL	0.04
Lenti-X™ Concentrator (Takara, 631232)	9 mL	16.09
Polybrene (Sigma-Aldrich™, TR-1003-G)	0,32 µL	0.02
Puromycin (Thermo Scientific Chemicals, J66301.MC)	4 µg	0.02
PrestoBlue® (Thermofisher, A13261)	450 µL	4.01
Matrigel (Corning, FAL356231)	6,4 mL	222.26
EC23 (Biotechne, 4011)	100 µL	6.42
Neurobasal-A-Media (Gibco™, 12348017)	250 mL	46
BDNF (Peprotech, 450-02)	500 µL	94.5
KCl (Sigma-Aldrich™, P5405)	100 µL	0
B27 (Gibco Life Technologies, 17564-044)	200 µL	2.14
Doxycycline (Thermo Scientific Chemicals, J67043.AE)	500 µL	1.1
Laminin (Gibco™, A29249)	500 µL	3.28
Acetic Acid (Sigma-Aldrich™, 338826)	2 mL	3.54
Bind Silane (Sigma-Aldrich™, 440159)	2 mL	1.18
Ethanol 96% (Panreac, 131085.1612)	100 mL	2.86
40% Acrylamide (Biorad, 161-0140)	4 mL	1.11
2% Bis Acrylamide (Biorad, 1610142)	1 mL	0.24
Beads (Invitrogen™, F8811)	72 µL	4.88
APS (Sigma-Aldrich™, A3678)	90 µL	0
TEMED (Sigma-Aldrich™, T9281-25ML)	9 µL	0.02
HEPES (Sigma-Aldrich™, H0887)	360 µL	0.63
Sulfo-SANPAH (Thermofisher)	3 mL	1.82
MilliQ Water (IBEC)	500 mL	2.5
Fibronectin (Gibco™, 33016015)	880 µL	2.9
4% PFA (Thermo Scientific Chemicals, 047392.9L)	10 mL	19
Triton X (Sigma-Aldrich™, T8787)	20 µL	0.02
2.5% BSA (Invitrogen™, A23017)	20 mL	11.04
Hoechst 33342 DNA stain	50 µL	1
MAP2 (Sigma-Aldrich™, MAB3418)	10 µL	0
b3 tubulin (Biolegend, 801201)	10 µL	68
SMI31 (Biolegend, 801601)	10 µL	27.6

NGN2 (Cellsignal, 13144S)	10 µL	31.3
YAP (Cellsignal, 14074S)	10 µL	36.4
TAU (Abcam, ab62639)	10 µL	54.5
Donkey anti-Ovine, Alexa Fluor™ 488 (Fisher, A-11015)	10 µL	0
Goat anti-mouse, Alexa Flour 488 conjugated (Thermofisher, A-11029)	10 µL	0
Donkey anti-mouse, Alexa Fluor™ 555 (Thermofisher, A-31570)	10 µL	0
Goat anti-Rabbit, Alexa Fluor 555 (Thermofisher, A-21429)	10 µL	0
One Use Material		
Sigma-Aldrich™ 10 µl pipette tips	200 units	5.45
Sigma-Aldrich™ 200 µl pipette tips	200 units	5.53
Sigma-Aldrich™ 1000 µl pipette tips	300 units	5.67
18 mm diameter coverslips (Paul Marienfield)	10 units	2.65
24 x 40 mm coverslips #1.5 (VWR) (Menzel-Gläser)	6 units	0.6
Sigma-Aldrich™ 2 ml serological pipettes	50 units	28.75
Sigma-Aldrich™ 5 ml serological pipettes	50 units	19.68
Sigma-Aldrich™ 10 ml serological pipettes	70 units	28.04
Sigma-Aldrich™ 25 ml serological pipettes	70 units	52.15
Sigma-Aldrich™ Eppendorf Conical tubes 1,5 mL	20 units	1.33
Sigma-Aldrich™ Eppendorf Conical tubes 0,5 mL	15 units	1.13
Sigma-Aldrich™ Corning 50 mL Centrifuge Tube	35 units	21
Sigma-Aldrich™ Corning 15 mL Centrifuge Tube	50 units	18.83
Sigma-Aldrich™ Cell culture flasks 75 cm2	20 units	45.8
Sigma-Aldrich™ Cell Culture 96-wells plate	4 units	13.13
Sigma-Aldrich™ Cell Culture 8 chamber slide	4 units	50
Sigma-Aldrich™ Cell Culture 6 wells plate	1 units	32.8
Sigma-Aldrich™ Microscope slide	10 units	14.72
Sigma-Aldrich™ Nitrile Santex Gloves	100 units	9.9
Cryovials	10 units	50
Equipment		
Neubauer chamber (BLAUBRAND®)	5 hours	0.05
Mr Frosty container	3 hours	0.06
Confocal Microscope (Zeiss LSM880)	10 hours	272
Biological culture hood (Telstar bio2 advance)	70 hours	5.32
Infinite M200 PRO Multimode Microplate Reader from Tescan	20 minutes	0.15
Cell culture inverted optical microscope (TS100; Nikon)	5 hours	0.11
Cell incubator (ThermoScientific forma steri-cycle i160)	4 months	466.6
Fridge (liebherr profiline)	4 months	31

Cell culture centrifuge (Eppendorf Centrifuge 5702)	3 h	0.16
Flow hood (flores valles)	10 h	0.32
Human Resources		
Undergraduate Student	370 h	2,160
Research Director	250 h	5,000
	TOTAL	**10,217.02 €**

The total price of the project ascends to 10,217.02€. The primary allocation of the budget is attributed to the acquisition of specialized laboratory reagents, particularly those essential for immunocytochemistry and differentiation procedures. These specific techniques need the utilization of specialized materials, which contributes significantly to the overall project expenses.

Nevertheless, it is noteworthy to highlight that the project has received funding and oversight from the IBEC, an established institution. As a result, the total expenditure may vary, as a substantial portion of the required materials is supplied by the institution or shared among various research endeavours.

9. REGULATION AND LEGAL ASPECTS

IBEC is fully committed to upholding the European Code of Conduct for Research Integrity [78], which underscores the fundamental principles of research integrity as the basis for good research practices. These principles encompass reliability, honesty, respect, and accountability. Also, as a public sector foundation, adheres to transparency standards set forth by the Charter of Fundamental Rights of the European Union [79] and the Spanish Transparency, Public Access to Information and Good Governance Law [80], which emphasizes transparency in public activities, ensures access to information, and promotes good governance practices. Nevertheless, The Spanish Law of Science, Technology, and Innovation of 2011 [81] also recognizes the importance of open access; so, publications must be accessible to the broader community, either through open access journals, open versions of regular journals, or by depositing them in public repositories.

Ethical considerations are paramount in research hence all activities within the institute adhere to fundamental ethical principles, national legislation, relevant EU legislation and standards, international conventions and directives, and the opinions of the European Group on Ethics and Protection of Animals. Specific regulations, such as EC Directive 86/609 [82], govern the ethical aspects of research involving animals. Moreover, the approval of national and local ethics committees is required before commencing any experiments, regarding research involving human embryonic material, IBEC abides by the current legislation in Spain, specifically Law 14/2007 on Biomedical Research [83] and Royal Decree 1527/2010 [84]. Researchers intending to work with pluripotent cell lines (hESCs/hiPSCs) must obtain approval from the competent authority, namely the Department of Health of the Government of Catalonia, for their research projects.

Also, some steps of the project involved the manipulation of potentially hazardous substances, biological agents, and human cells, specifically, PFA and SH-SY5Y tumour cells. Consequently, being aware of the regulations established by the European Commission and the Spanish Government was crucial. Directive 2000/54/EC of the European Parliament and the Council of 18 September 2000 [85] gives the guidelines to ensure safety and protection from hazards associated with exposure to biological agents in the workplace. In Spain, this concern is also regulated by the Royal Decree Law 664/1997 [86] which further classifies biological agents.

The Institute of Bioengineering of Catalonia also hosted a complete training course on proper laboratory practices, which was compulsory before using the laboratory facilities. This instruction included a thorough explanation of Spanish Law 31/1995 [87], which focuses on preventing occupational risks and how to apply it in lab settings. Through this training, participants gained the skills and practises needed to safely manage biological and chemical samples, dispose of laboratory waste properly, and react to an accident.

10. CONCLUSIONS AND FUTURE LINES

Our results state that NGN2 induction is an efficient way to induce neuronal pseudo differentiation of SH-SY5Y cells. In the relatively short period of 10 days, NGN2 allows the cells to acquire a more mature phenotype efficiently and consistently, with better morphological features and improved expression and distribution of the markers analysed. Nonetheless, it is important to acknowledge that with our timeframe and protocol, the SH-SY5Y cells did not fully establish a clear compartmentalization between the soma and axon. Despite the evident enhancement of neuronal commitment through NGN2 overexpression, the observed lack of complete soma-axon compartmentalization for MAP2 and TAU suggests that further steps are necessary to achieve a more refined and distinct neuronal phenotype, which can be a necessary requirement for their use as a preclinical model. This observation raises the possibility that additional factors or extended culture conditions may be required to facilitate a more advanced stage of neuronal development. Future investigations should aim to address this aspect, exploring various strategies such as the modulation of other neuronal master genes or the optimization of culture conditions.

Moreover, if the differentiation method described in this study is used for preclinical or basic research purposes in the future, a more extensive characterization of the generated cells would be necessary, including the incorporation of additional markers for specific neuronal types. This is important because the SH-SY5Y cells have the potential to differentiate into various neuronal subtypes, and a comprehensive analysis would allow us to determine which neuronal type they closely resemble [88]. This research also holds promise for their use to better understand diverse neurodegenerative disorders, such as Parkinson's disease (by inducing differentiation into pseudo-dopaminergic neurons) or Huntington's disease.

Furthermore, our results prove the mechanosensitivity of these neuronal-type cells and their plasticity in response to substrate stiffness, both at a morphological and at a signalling pathway level. We have demonstrated that SH-SY5Y have detectable expression levels of YAP, and its nucleo-cytoplasmic localization is mechanoreulated. Notably, under conditions inducing higher cellular tension (i.e., high stiffness), YAP cofactor accumulates within the nucleus, where it can exert its co-transcriptional activity, regulating fundamental genes for cell survival and behaviour. Our findings indicate that cells showed a morphology more compatible with typical neuronal shape when cultured onto stiffer matrices, which seems counterintuitive given that the brain is a very soft organ. Literature calculations of brain stiffness go from around 2 kPa to less than 1 kPa [89]. This apparent incongruity between the natural stiffness of the brain and the preferred stiffness observed in vitro can be attributed to the multiscale mechanical properties of brain, which can display disparity between bulk (macroscopic stiffness) and the microscopic-scale stiffness experienced by neurons. For example, while hyaluronic acid network, the main structural component of the brain, is very soft, neurons are surrounded by synapses, with an estimated stiffness of around 200 kPa [90].

The importance of our finding relies on the capacity to link the changes in brain stiffness and the alternation in the expression/activity of YAP during neurodegenerative diseases. It has been described so far, the mechanical properties of the brain undergo alterations during aging and disease, with a progressing softening [91]. We demonstrated that neuronal YAP is indeed able to respond to the environmental mechanical cues, and therefore, could be at least partially responsible for changes in neuronal behaviour during the alterations of the mechanical properties of the brain. This opens the door to the development of new strategies targeting YAP activity, bringing the emerging field of mechanotherapeutics [92] a step closer to neurodegenerative diseases such as Alzheimer's disease.

11. REFERENCES

[1] Kamkin, A. (2005g) Mechanosensitivity of Cells from Various Tissues. Available at: https://www.ncbi.nlm.nih.gov/books/NBK7493/.

[2] Institute for Bioengineering of Catalonia (2023b) Cellular and molecular mechanobiology - Institute for Bioengineering of Catalonia. Available at: https://ibecbarcelona.eu/cellmolmech.

[3] Adminpcb (2022b) Contact - Parc Científic de Barcelona. Available at: https://www.pcb.ub.edu/en/contact/.

[4] Cimler, R. et al. (2019b) "Predictions of Alzheimer's disease treatment and care costs in European countries," PLOS ONE, 14(1), p. e0210958. Available at: https://doi.org/10.1371/journal.pone.0210958.

[5] Iqbal, K. et al. (2010b) "Tau in Alzheimer Disease and Related Tauopathies," Current Alzheimer Research, 7(8), pp. 656–664. Available at: https://doi.org/10.2174/156720510793611592.

[6] Shively, S.B. et al. (2012c) "Dementia Resulting From Traumatic Brain Injury," Archives of Neurology, 69(10). Available at: https://doi.org/10.1001/archneurol.2011.3747.

[7] Totaro, A. et al. (2017b) "YAP/TAZ link cell mechanics to Notch signalling to control epidermal stem cell fate," Nature Communications, 8(1). Available at: https://doi.org/10.1038/ncomms15206.

[8] Rojek, K. et al. (2019b) "Amot and Yap1 regulate neuronal dendritic tree complexity and locomotor coordination in mice," PLOS Biology, 17(5), p. e3000253. Available at: https://doi.org/10.1371/journal.pbio.3000253.

[9] Shimizu, T. et al. (2017b) "YAP functions as a mechanotransducer in oligodendrocyte morphogenesis and maturation," Glia, 65(2), pp. 360–374. Available at: https://doi.org/10.1002/glia.23096.

[10] Tekin, H. et al. (2018b) "Effects of 3D culturing conditions on the transcriptomic profile of stem-cell-derived neurons," Nature Biomedical Engineering, 2(7), pp. 540–554. Available at: https://doi.org/10.1038/s41551-018-0219-9.

[11] Shively, S.B. et al. (2012d) "Dementia Resulting From Traumatic Brain Injury," Archives of Neurology, 69(10). Available at: https://doi.org/10.1001/archneurol.2011.3747.

[12] King, A.I. et al. (1995b) "Recent Advances in Biomechanics of Brain Injury Research: A Review," Journal of Neurotrauma, 12(4), pp. 651–658. Available at: https://doi.org/10.1089/neu.1995.12.651.

[13] Kleiven, S. (2007b) "Predictors for traumatic brain injuries evaluated through accident reconstructions," ResearchGate [Preprint]. Available at: https://www.researchgate.net/publication/5572726.

[14] Andrews, M.R. et al. (2016b) "Axonal Localization of Integrins in the CNS Is Neuronal Type and Age Dependent," ENeuro, 3(4), p. ENEURO.0029-16.2016. Available at: https://doi.org/10.1523/eneuro.0029-16.2016.

[15] Sydor, A.M. et al. (1996b) "Talin and vinculin play distinct roles in filopodial motility in the neuronal growth cone.," Journal of Cell Biology, 134(5), pp. 1197–1207. Available at: https://doi.org/10.1083/jcb.134.5.1197.

[16] Xu, Z.S. et al. (2013b) "Evidence of Changes in Brain Tissue Stiffness After Ischemic Stroke Derived From Ultrasound-Based Elastography," Journal of Ultrasound in Medicine, 32(3), pp. 485–494. Available at: https://doi.org/10.7863/jum.2013.32.3.485.

[17] Kubitschke, H. et al. (2017b) "Actin and microtubule networks contribute differently to cell response for small and large strains," New Journal of Physics, 19(9), p. 093003. Available at: https://doi.org/10.1088/1367-2630/aa7658.

[18] Case, N. et al. (2011b) "Mechanical Regulation of Glycogen Synthase Kinase 3β (GSK3β) in Mesenchymal Stem Cells Is Dependent on Akt Protein Serine 473 Phosphorylation via mTORC2 Protein," Journal of Biological Chemistry, 286(45), pp. 39450–39456. Available at: https://doi.org/10.1074/jbc.m111.265330.

[19] Kobayakawa, T. et al. (2016b) "Mechanical stress loading induces CD44 cleavage in human chondrocytic HCS-2/8 cells," Biochemical and Biophysical Research Communications, 478(3), pp. 1230–1235. Available at: https://doi.org/10.1016/j.bbrc.2016.08.099.

[20] Kruger, T.M. et al. (2019c) "Reduced Extracellular Matrix Stiffness Prompts SH-SY5Y Cell Softening and Actin Turnover To Selectively Increase Aβ(1–42) Endocytosis," ACS Chemical Neuroscience, 10(3), pp. 1284–1293. Available at: https://doi.org/10.1021/acschemneuro.8b00366.

[21] Spencer, K. et al. (2017) "A three dimensional in vitro glial scar model to investigate the local strain effects from micromotion around neural implants," Lab on a Chip, 17(5), pp. 795–804. Available at: https://doi.org/10.1039/c6lc01411a.

[22] Spencer, K. et al. (2017b) "A three dimensional in vitro glial scar model to investigate the local strain effects from micromotion around neural implants," Lab on a Chip, 17(5), pp. 795–804. Available at: https://doi.org/10.1039/c6lc01411a.

[23] Tanaka, H. et al. (2020) "YAP-dependent necrosis occurs in early stages of Alzheimer's disease and regulates mouse model pathology," Nature Communications, 11(1). Available at: https://doi.org/10.1038/s41467-020-14353-6.

[24] Boder, E.J. and Banerjee, I.A. (2021) "Alzheimer's Disease: Current Perspectives and Advances in Physiological Modeling," Bioengineering, 8(12), p. 211. Available at: https://doi.org/10.3390/bioengineering8120211.

[25] Drummond, E. and Wisniewski, T. (2017b) "Alzheimer's disease: experimental models and reality," Acta Neuropathologica, 133(2), pp. 155–175. Available at: https://doi.org/10.1007/s00401-016-1662-x.

[26] Prasanna, P. et al. (2021) "Microfluidic Platforms to Unravel Mysteries of Alzheimer's Disease: How Far Have We Come?," Life, 11(10), p. 1022. Available at: https://doi.org/10.3390/life11101022.

[27] Krishna, A. et al. (2014) "Systems genomics evaluation of the SH-SY5Y neuroblastoma cell line as a model for Parkinson's disease," BMC Genomics, 15(1), p. 1154. Available at: https://doi.org/10.1186/1471-2164-15-1154.

[28] Hall, C.M., Moeendarbary, E. and Sheridan, G.K. (2021b) "Mechanobiology of the brain in ageing and Alzheimer's disease," European Journal of Neuroscience, 53(12), pp. 3851–3878. Available at: https://doi.org/10.1111/ejn.14766.

[29] Tortorella, I. et al. (2022b) "Biochemical Pathways of Cellular Mechanosensing/Mechanotransduction and Their Role in Neurodegenerative Diseases Pathogenesis," Cells, 11(19), p. 3093. Available at: https://doi.org/10.3390/cells11193093.

[30] Bell, M.G.H. and Zempel, H. (2021) "SH-SY5Y-derived neurons: a human neuronal model system for investigating TAU sorting and neuronal subtype-specific TAU vulnerability," Reviews in the Neurosciences, 33(1), pp. 1–15. Available at: https://doi.org/10.1515/revneuro-2020-0152.

[31] Shih, P.C. et al. (2021) "Development of a fully human assay combining NGN2-inducible neurons co-cultured with iPSC-derived astrocytes amenable for electrophysiological studies," Stem Cell Research, 54, p. 102386. Available at: https://doi.org/10.1016/j.scr.2021.102386.

[32] Lin, H.-C. et al. (2021) "NGN2 induces diverse neuron types from human pluripotency," Stem Cell Reports, 16(9), pp. 2118–2127. Available at: https://doi.org/10.1016/j.stemcr.2021.07.006.

[33] Hulme, A.J. et al. (2021) "Making neurons, made easy: The use of Neurogenin-2 in neuronal differentiation," Stem Cell Reports, 17(1), pp. 14–34. Available at: https://doi.org/10.1016/j.stemcr.2021.11.015.

[34] Zhou, X.K. et al. (2006) "Optimization of the Tet-On system for regulated gene expression through viral evolution," Gene Therapy, 13(19), pp. 1382–1390. Available at: https://doi.org/10.1038/sj.gt.3302780.

[35] Das, A.T., Tenenbaum, L. and Berkhout, B. (2016) "Tet-On Systems For Doxycycline-inducible Gene Expression," Current Gene Therapy, 16(3), pp. 156–167. Available at: https://doi.org/10.2174/1566523216666160524144041.

[36] World Alzheimer Report 2022: Life after diagnosis: Navigating treatment, care and support (2022). Available at: https://www.alzint.org/resource/world-alzheimer-report-2022/.

[37] Alzheimer's Therapeutics Market Statistics and Forecast - 2031 (no date). Available at: https://www.alliedmarketresearch.com/alzheimers-therapeutics-market-A10535.

[38] Gustavsson, A. et al. (2022) "Global estimates on the number of persons across the Alzheimer's disease continuum," Alzheimers & Dementia, 19(2), pp. 658–670. Available at: https://doi.org/10.1002/alz.12694.

[39] Castellani, R.J., Rolston, R.K. and Smith, M.A. (2010) "Alzheimer Disease," Dm Disease-a-month, 56(9), pp. 484–546. Available at: https://doi.org/10.1016/j.disamonth.2010.06.001.

[40] Brookmeyer, R. et al. (2007) "Forecasting the global burden of Alzheimer's disease," Alzheimers & Dementia, 3(3), pp. 186–191. Available at: https://doi.org/10.1016/j.jalz.2007.04.381.

[41] Ramírez-Bermúdez, J. (2012) "Alzheimer's Disease: Critical Notes on the History of a Medical Concept," Archives of Medical Research, 43(8), pp. 595–599. Available at: https://doi.org/10.1016/j.arcmed.2012.11.008.

[42] Yang, H.K. et al. (2016) "History of Alzheimer's Disease," Dementia and Neurocognitive Disorders, 15(4), p. 115. Available at: https://doi.org/10.12779/dnd.2016.15.4.115.

[43] Atri, A. (2019) "Current and Future Treatments in Alzheimer's Disease," Seminars in Neurology, 39(02), pp. 227–240. Available at: https://doi.org/10.1055/s-0039-1678581.

[44] Yiannopoulou, K.G. and Papageorgiou, S.G. (2020) "Current and Future Treatments in Alzheimer Disease: An Update," Journal of Central Nervous System Disease, 12, p. 117957352090739. Available at: https://doi.org/10.1177/1179573520907397.

[45] Nilsson, P., Saito, T. and Saido, T.C. (2014) "New Mouse Model of Alzheimer's," ACS Chemical Neuroscience, 5(7), pp. 499–502. Available at: https://doi.org/10.1021/cn500105p.

[46] Pippin, J.J. (no date) Animal Research for Alzheimer Disease: Failures of Science and Ethics. Available at: https://www.wellbeingintlstudiesrepository.org/bioamres/15/.

[47] Qin, T. et al. (2020) "Utility of Animal Models to Understand Human Alzheimer's Disease, Using the Mastermind Research Approach to Avoid Unnecessary Further Sacrifices of Animals," International Journal of Molecular Sciences, 21(9), p. 3158. Available at: https://doi.org/10.3390/ijms21093158.

[48] Dubey, S.K. et al. (2019) "Recent Expansions on Cellular Models to Uncover the Scientific Barriers Towards Drug Development for Alzheimer's Disease," Cellular and Molecular Neurobiology, 39(2), pp. 181–209. Available at: https://doi.org/10.1007/s10571-019-00653-z.

[49] Alipour, M.A. et al. (2019) "Stem cell therapy in Alzheimer's disease: possible benefits and limiting drawbacks," Molecular Biology Reports, 46(1), pp. 1425–1446. Available at: https://doi.org/10.1007/s11033-018-4499-7.

[50] Dravid, A. et al. (2021) "Optimised techniques for high-throughput screening of differentiated SH-SY5Y cells and application for neurite outgrowth assays," Scientific Reports, 11(1). Available at: https://doi.org/10.1038/s41598-021-03442-1.

[51] Overbaugh, J., Mangold, C.A., and Szpara, M.L. (2016) "Differentiation of the SH-SY5Y Human Neuroblastoma Cell Line," Journal of Visualized Experiments [Preprint], (108). Available at: https://doi.org/10.3791/53193.

[52] Christie, V.B. et al. (2010) "Retinoid supplementation of differentiating human neural progenitors and embryonic stem cells leads to enhanced neurogenesis in vitro," Journal of Neuroscience Methods, 193(2), pp. 239–245. Available at: https://doi.org/10.1016/j.jneumeth.2010.08.022.

[53] Clemens, G. et al. (2013) "The action of all-trans-retinoic acid (ATRA) and synthetic retinoid analogues (EC19 and EC23) on human pluripotent stem cells differentiation investigated using single cell infrared microspectroscopy," Molecular BioSystems, 9(4), p. 677. Available at: https://doi.org/10.1039/c3mb25505k.

[54] Dwane, S., Durack, E. and Kiely, P.A. (2013) "Optimising parameters for the differentiation of SH-SY5Y cells to study cell adhesion and cell migration," BMC Research Notes, 6(1). Available at: https://doi.org/10.1186/1756-0500-6-366.

[55] Xu, M., McCanna, D.J. and Sivak, J.G. (2015) "Use of the viability reagent PrestoBlue in comparison with alamarBlue and MTT to assess the viability of human corneal epithelial cells," Journal of Pharmacological and Toxicological Methods, 71, pp. 1–7. Available at: https://doi.org/10.1016/j.vascn.2014.11.003.

[56] Halpain, S. and Dehmelt, L. (2006) "The MAP2/Tau family of microtubule-associated proteins," GenomeBiology.com (London. Print), 6(1), p. 204. Available at: https://doi.org/10.1186/gb-2004-6-1-204.

[57] Francis, F. et al. (1999) "Doublecortin Is a Developmentally Regulated, Microtubule-Associated Protein Expressed in Migrating and Differentiating Neurons," Neuron, 23(2), pp. 247–256. Available at: https://doi.org/10.1016/s0896-6273(00)80777-1.

[58] Lee, M.D. et al. (1990) "The expression and posttranslational modification of a neuron-specific ß-tubulin isotype during chick embryogenesis," Cell Motil Cytoskeleton, 17(2), pp. 118–132. Available at: https://doi.org/10.1002/cm.970170207.

[59] Khalil, M. et al. (2018) "Neurofilaments as biomarkers in neurological disorders," Nature Reviews Neurology, 14(10), pp. 577–589. Available at: https://doi.org/10.1038/s41582-018-0058-z.

[60] Yuan, A. et al. (2012) "Neurofilaments at a glance," Journal of Cell Science, 125(14), pp. 3257–3263. Available at: https://doi.org/10.1242/jcs.104729.

[61] Pooler, A.M. and Hanger, D.P. (2010) "Functional implications of the association of tau with the plasma membrane," Biochemical Society Transactions, 38(4), pp. 1012–1015. Available at: https://doi.org/10.1042/bst0381012.

[62] Sensenbrenner, M., Lucas, M. and Deloulme, J.-C. (1997) "Expression of two neuronal markers, growth-associated protein 43 and neuron-specific enolase, in rat glial cells," Journal of Molecular Medicine, 75(9), pp. 653–663. Available at: https://doi.org/10.1007/s001090050149.

[63] Fraga, D., Meulia, T. and Fenster, S.D. (2008) "Real-Time PCR," Current Protocols Essential Laboratory Techniques, 00(1). Available at: https://doi.org/10.1002/9780470089941.et1003s00.

[64] Valasek, M.A. and Repa, J.J. (2005) "The power of real-time PCR," Advances in Physiology Education, 29(3), pp. 151–159. Available at: https://doi.org/10.1152/advan.00019.2005.

[65] Burry, R.W. (2011b) "Controls for Immunocytochemistry," Journal of Histochemistry and Cytochemistry, 59(1), pp. 6–12. Available at: https://doi.org/10.1369/jhc.2010.956920.

[66] Ozgun, A. et al. (2021) "Substrate stiffness effects on SH-SY5Y : The dichotomy of morphology and neuronal behavior," Journal of Biomedical Materials Research Part B, 109(1), pp. 92–101. Available at: https://doi.org/10.1002/jbm.b.34684.

[67] Lau, L. et al. (2013) "Pathophysiology of the brain extracellular matrix: a new target for remyelination," Nature Reviews Neuroscience, 14(10), pp. 722–729. Available at: https://doi.org/10.1038/nrn3550.

[68] Zhao, B. et al. (2010) "The Hippo–YAP pathway in organ size control and tumorigenesis: an updated version," Genes & Development, 24(9), pp. 862–874. Available at: https://doi.org/10.1101/gad.1909210.

[69] Hilman, D. and Gat, U. (2011) "The Evolutionary History of YAP and the Hippo/YAP Pathway," Molecular Biology and Evolution, 28(8), pp. 2403–2417. Available at: https://doi.org/10.1093/molbev/msr065.

[70] Dobson, E.T.A. et al. (2021) "ImageJ and CellProfiler: Complements in Open-Source Bioimage Analysis," Current Protocols, 1(5). Available at: https://doi.org/10.1002/cpz1.89.

[71] Lamprecht, M.R., Sabatini, D.M. and Carpenter, A.E. (2007) "CellProfilerTM: free, versatile software for automated biological image analysis," BioTechniques, 42(1), pp. 71–75. Available at: https://doi.org/10.2144/000112257.

[72] Collins, T. (2007) "ImageJ for microscopy," BioTechniques, 43(1S), pp. S25–S30. Available at: https://doi.org/10.2144/000112517.

[73] Lee, K. and Nelson, C.M. (2013) "Determining the Role of Matrix Compliance in the Differentiation of Mammary Stem Cells," in Springer eBooks, pp. 79–94. Available at: https://doi.org/10.1007/7651_2013_31.

[74] Kim, M.C. et al. (2013) "cAMP/PKA signalling reinforces the LATS–YAP pathway to fully suppress YAP in response to actin cytoskeletal changes," The EMBO Journal, 32(11), pp. 1543–1555. Available at: https://doi.org/10.1038/emboj.2013.102.

[75] Shea, T.B. et al. (1988) "Soluble, phosphorylated forms of the high molecular weight neurofilament protein in perikarya of cultured neuronal cells," Neuroscience Letters, 92(3), pp. 291–297. Available at: https://doi.org/10.1016/0304-3940(88)90605-2.

[76] Mata, M. (1992) Phosphorylation-dependent neurofilament epitopes are reduced at the node of Ranvier. Available at: https://deepblue.lib.umich.edu/handle/2027.42/47426.

[77] Fischer, I. et al. (1986) "Expression and distribution of microtubule-associated protein 2 (MAP2) in neuroblastoma and primary neuronal cells," Developmental Brain Research, 25(1), pp. 99–109. Available at: https://doi.org/10.1016/0165-3806(86)90156-2.

[78] ALLEA (2023b) The European Code of Conduct for Research Integrity - ALLEA. Available at: https://allea.org/code-of-conduct/.

[79] EU, E. (2012). "Charter of fundamental rights of the European Union," The Review of International Affairs, 63(1147), 109-123. Available at: https://www.europarl.europa.eu/charter/pdf/text_en.pdf

[80] Spain. Act 19/2013, of 9 December, on Transparency, Access to Public Information, and Good Governance. Boletín Oficial del Estado, 9th of December of 2013, num. 295. Available at: https://www.hacienda.gob.es/Documentacion/Publico/AdministracionElectronica/Act-19-2013_on_transparency_access_to_public_information_and_good_governance.pdf

[81] Act 14/2011, of 1 June, on Science, Technology, and Innovation. Boletín Oficial del Estado, 1st of June of 2011, num. 131. Available at: https://www.boe.es/buscar/act.php?id=BOE-A-2011-9617

[82] 'Directiva 86/609/CEE del Consejo de 24 de noviembre de 1986 relativa a la aproximación de las disposiciones legales, reglamentarias y administrativas de los Estados Miembros respecto a la protección de los animales utilizados para experimentación y otros fines científicos' (1986) Official Journal L 358, 1-28. http://data.europa.eu/eli/dir/1986/609/oj

[83] Law 14/2007, of 3 July, on Biomedical Research. Boletín Oficial del Estado, 4th of July of 2007, num. 159. Available at: https://www.boe.es/buscar/doc.php?id=BOE-A-2007-12945

[84] Royal Decree 1090/2015, of 4 December, regulating clinical trials with medicinal products, Ethics Committees for Investigation with medicinal products and the Spanish Clinical Studies Registry. Boletín Oficial del Estado, 25th of December of 2015, num. 307, pp 121923-121964. Available at: https://www.boe.es/buscar/doc.php?id=BOE-A-2015-14082

[85] Official Journal. Directive 2000/54/EC of the European Parliament and of the Council of 18 September 2000 on the Protection of Workers from Risks related to Exposure to Biological Agents at Work. Official Journal, 18 September 2020; 25. Available at: https://www.boe.es/buscar/doc.php?id=DOUE-L-2000-81929

[86] Royal Decree 664/1997, 12 May 1997, on the protection of workers against risks related to exposure to biological agents at work. Boletín del Estado, 24th of May of 1997, num. 124. Available at: https://www.boe.es/buscar/act.php?id=BOE-A-1997-11144

[87] Act 31/1995, of 8 November 1995, on the prevention of occupational hazards. Boletín del Estado, 10th of November of 1995, num. 269. Available at: https://www.boe.es/buscar/act.php?id=BOE-A-1995-24292

[88] Bell, M.G.H. and Zempel, H. (2021b) "SH-SY5Y-derived neurons: a human neuronal model system for investigating TAU sorting and neuronal subtype-specific TAU vulnerability," Reviews in the Neurosciences, 33(1), pp. 1–15. Available at: https://doi.org/10.1515/revneuro-2020-0152.

[89] Yin, Z. et al. (2018) "Stiffness and Beyond," Topics in Magnetic Resonance Imaging, 27(5), pp. 305–318. Available at: https://doi.org/10.1097/rmr.0000000000000178.

[90] Yang, J.D. et al. (2020) "Extreme stiffness of neuronal synapses and implications for synaptic adhesion and plasticity," bioRxiv (Cold Spring Harbor Laboratory) [Preprint]. Available at: https://doi.org/10.1101/2020.08.31.273466.

[91] Hiscox, L.V. et al. (2021) "Aging brain mechanics: Progress and promise of magnetic resonance elastography," NeuroImage, 232, p. 117889. Available at: https://doi.org/10.1016/j.neuroimage.2021.117889.

[92] Tschumperlin, D.J. and Lagares, D. (2020) "Mechano-therapeutics: Targeting Mechanical Signaling in Fibrosis and Tumor Stroma," Pharmacology & Therapeutics, 212, p. 107575. Available at: https://doi.org/10.1016/j.pharmthera.2020.107575.

12. ANNEXES

Annex 1: Cell Culture Protocols

SH-SY5Y Medium Protocol

1. Prepare a filtering kit and place a 500 ml glass bottle into it.
2. Combine 56 mL of FBS (inactivated) and 5,6 mL of Pen/Strep*L-Glut, on top of the filter.
3. Slowly add DMEM/F12 to the mixture until the total volume reaches 500 ml.
4. Connect the vacuum to the filtering kit and securely close the lid.

SH-SY5Y Thawing Protocol

1. Retrieve the cryovial containing frozen SH-SY5Y cells from the liquid nitrogen tank.
2. Place the cryovial in a 37°C water bath until the contents are nearly thawed.
3. Clean the exterior of the cryovial, including the cap, with 70% ethanol to ensure sterility, and transfer it to the sterile culture hood.
4. Dilute the contents of the cryovial in 6 ml of pre-warmed culture medium.
5. Centrifuge the diluted cell suspension at 300 x g for 5 minutes to pellet the cells.
6. Gently resuspend the cell pellet in the desired volume of culture medium and proceed with cell seeding according to the experimental requirements.

SH-SY5Y Freezing Protocol

1. Detach the SH-SY5Y cells as per the established method.
2. Resuspend the cell pellet in 1 mL of appropriate cell medium.
3. Prepare the necessary dilutions to achieve a final volume of 1 mL per cryovial, with a composition of 90% cell medium and 10% DMSO.
4. Transfer 1 mL of the cell suspension into each cryovial promptly, ensuring proper sealing of the cryovials.
5. Place all cryovials in a Mr. Frosty container and promptly store them at -80°C for 24 hours.
6. After 24 hours, transfer the cryovials to a liquid nitrogen storage tank for long-term preservation.

SH-SY5Y passaging Protocol

For each T75 flask with cells at 90% confluency:

1. Remove the cell culture medium and rinse the cells with PBS, allowing them to incubate in PBS for 5 minutes at RT.
2. Aspirate the PBS and add 1 ml of TrypLE Express™ to the flask.
3. Incubate the flask in the cell incubator for 5 minutes.
4. Add 5 ml of cell medium or PBS to the flask and transfer the contents to a 15 ml centrifuge tube.

5. Prepare a filtering kit and place a 500 ml glass bottle into it.
6. Combine 56 mL of FBS (inactivated) and 5,6 mL of Pen/Strep*L-Glut, on top of the filter.
7. Slowly add DMEM/F12 to the mixture until the total volume reaches 500 ml.
8. Connect the vacuum to the filtering kit and securely close the lid.

Cell Counting Protocol

Adapted from

1. Clean the haemocytometer thoroughly using 70% ethanol to ensure sterility before use.
2. Follow the cell detachment procedure outlined in Annex 1.4 to detach the cells.
3. Take 10 µl of the cell solution and dilute it in 90 µl of cell medium, resulting in a 1:10 dilution.
4. In a separate tube, mix 10 µl of the diluted cell solution with 10 µl of trypan blue. Ensure thorough mixing.
5. Carefully add 10 µl of the mixed sample to the grid area between the coverslip and counting chamber of the haemocytometer, as shown in the image below. Take care not to overfill the chamber but allow the sample to reach the edges of the grooves. Repeat the process for the second chamber if necessary.
6. Place the Neubauer chamber on the microscope stage and ensure it is securely in place. Adjust the microscope focus until a clear image of the cells is visible when looking through the eyepiece and adjusting the stage.
7. Locate the first counting grid square where the cell count will begin. Start counting the cells within this square using the appropriate magnification. Note the number of cells present within the square.
8. Repeat the counting process for the remaining 4 squares located in the corners of the counting grid, as indicated in the provided image. Count the cells within each square and record the respective cell numbers.

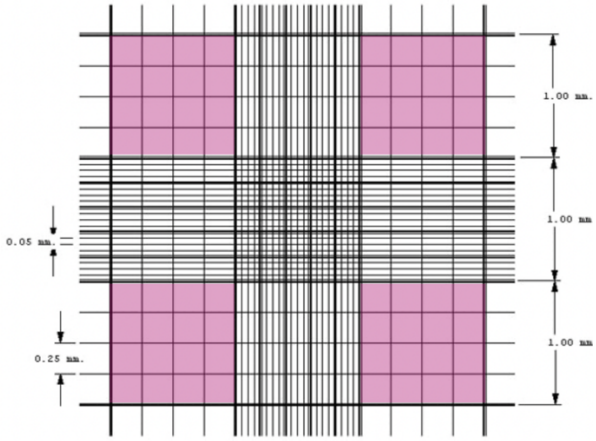

9. The total concentration will be calculated using the following formula.

$$Concentration = \frac{Number\ of\ Cells \cdot 10000}{Number\ of\ square \cdot dilution}$$

Annex 2: Lentivirus transfection

Reagents:

- Plasmid of interest (NGN2)
- Packaging plasmids:
- pMD2.G
- psPAX2
- HEK 293T cells
- Lipofectamine 3000/P3000 reagent
- OptiMEM
- Normal medium for HEK cells: DMEM High glucose + 1X Glutamine + 1X Pen/Strep
- Lenti-X™ Concentrator
- Polybrene
- Puromycin (1 µg/ml)

Protocol:

Lentiviral Production

Day 0:

1. Culture HEK 293T cells in normal medium to achieve 40-50% confluence. Passage the cells the night before or in the morning prior to the protocol to minimize colony growth. Seeding 3-4 million cells 24 hours before is sufficient and avoids the need for passage the following day.

Day 1:

1. Change the medium of HEK 293T cells to new medium containing serum approximately 1 hour before transfection.
2. Equilibrate OptiMEM and Lipofectamine 3000/P3000 reagent aliquots at room temperature.
3. Dilute the plasmids in 500 µL of OptiMEM and vortex-spin.
   a) Plasmid of interest: 5000 ng
   b) pMD2.G: 1750 ng
   c) psPAX2: 3250 ng
4. Add 20 µL of P3000 reagent.
5. In a separate Eppendorf tube, mix 30 µL of Lipofectamine 3000 with 500 µL of OptiMEM, vortex-spin.
6. Combine the Lipofectamine mix with the plasmids and P3000 reagent. Mix by inversion, avoiding foam formation, and incubate for 15 minutes at room temperature.
7. Apply the transfection mixture dropwise to the HEK 293T cells.
8. Incubate overnight.

Day 2:

1. Change the medium of the transfected HEK 293T cells.

Day 3 & Day 4:

1. Check the cells to ensure they remain attached.
2. Collect approximately 10 mL of medium, centrifuge at 500 × g for 10 minutes at 4°C to remove cell debris and add fresh medium to the cells.
3. Filter the collected medium using a 0.45 µm syringe filter.
4. Store the filtered medium at +4ºC, covered with parafilm.

Day 5:

1. Collect approximately 10 mL of medium, centrifuge at 500 × g for 10 minutes at 4°C, and discard cells following safety protocols.
2. Filter the collected medium using a 0.45 µm syringe filter.
3. Mix the filtered medium with the supernatant collected from Day 1 and Day 2. If concentration is planned, it is advisable to combine all supernatants.

Lentiviral Concentration with Lenti-X

1. Transfer the clarified supernatant to a sterile 50 mL Falcon tube.
2. Combine 1 volume of Lenti-X Concentrator with 3 volumes of the clarified supernatant.
3. Incubate the mixture at 4°C for 30 minutes to overnight (recommended at least 2 hours) to allow precipitation. Ensure that the supernatant from Days 1 and 2 has been refrigerated, and Lenti-X has been stored in the fridge.
4. Centrifuge the sample at 1,500 × g for 45 minutes at 4°C. An off-white pellet will form.
5. Carefully remove the supernatant without disturbing the pellet. Residual supernatant can be removed by pipette tip or brief centrifugation at 1,500 × g.
6. Gently resuspend the pellet in 1/10th to 1/100th of the original volume using complete DMEM, PBS, or TNE. Initially, the pellet may be sticky but will quickly go into suspension.
7. Store the concentrated lentivirus at +4°C or use immediately.

Infection

1. Prepare a solution of Polybrene + lentivirus using normal medium.
2. Apply the equivalent of 4 mL to a 25 cm² flask of Sh-SY5Y cells.
3. Add Polybrene to achieve a final concentration of 8 µg/mL.
4. Apply the solution dropwise to the cells and incubate overnight.
5. Change to normal medium the following morning.

Cell Selection

1. After 48 hours, change the medium to contain Puromycin at a concentration of 1 µg/mL.
2. Non-transfected cells will undergo cell death within 48-72 hours.

Annex 3: PrestoBlue Cell Viability Study Protocol

Required reagents and equipment:

- Cell Culture Media
- PrestoBlue® reagent
- Infinite M200 PRO Multimode Microplate Reader from Tescan

Procedure:

1. Seed the desired number of cells into a 96-well plate.
2. Change the medium in the wells 24 hours before starting the experiment.
3. Prepare a reservoir with PrestoBlue reagent.
4. Using a multipipette, dispense 10 µL of PrestoBlue reagent into each well of the plate.
5. Incubate the plate in a 37-degree Celsius incubator for 2 hours.
6. After incubation, place the plate in the plate reader and set the excitation wavelength to 560 nm and emission wavelength to 590 nm for bottom-read fluorescence measurement.
7. Set the plate reader to automatic sensitivity.
8. Read the fluorescence of each well in the plate using the plate reader.

Annex 4: Differentiation of SH-SY5Y into pseudo neurons

Protocol obtained from: Dravid, A. et al. (2021b) "Optimised techniques for high-throughput screening of differentiated SH-SY5Y cells and application for neurite outgrowth assays," Scientific Reports, 11(1). Available at: https://doi.org/10.1038/s41598-021-03442-1.

Reagents

- Dulbecco's Modified Eagle's Medium (DMEM)
- Heat-inactivated fetal bovine serum (hiFBS)
- Glutamax-I
- Penicillin/streptomycin
- Matrigel (1:100 dilution)
- Retinoic acid (RA)
- Neurobasal-A media
- Brain-derived neurotrophic factor (BDNF)
- Potassium chloride (KCl)
- B27

Procedure

1. Seed cells onto Matrigel-coated (1:100) dishes at specified densities relevant to the experiment.
2. The following day, change the medium to Stage I medium which includes DMEM supplemented with hiFBS (2.5%), 1 × glutamax-I, 1 × penicillin/streptomycin, Retinoic acid (RA) (10 μM).
3. After five days, change the medium to Stage II medium made out of Neurobasal-A medium supplemented with Brain-derived neurotrophic factor (BDNF) (50 ng/mL), Potassium chloride (KCl) (20 mM), 1 × B27, 1 × glutamax-I, 1 × penicillin/streptomycin.
4. After an additional five days, cells are considered to be differentiated.

Notes: Cultivated cells should be maintained below passage 12 and at a temperature of 37 °C with 5% CO2.

Annex 5: Gel preparation and functionalization

List of materials and location

- Acetic acid
- Bind Silane
- Ethanol 96%
- 1x PBS
- 40% acrylamide
- 2% Bis acrylamide
- Beads
- APS
- TEMED
- HEPES
- NHS
- Irgacure
- Tetracrylate
- MilliQ
- Fibronectin
- Cover glass

Procedure

Glass treatment

1. In a mixing container, combine 714 µl of Acetic Acid and 714 µl of Bind Silane.
2. Add ethanol 96% to the mixture, filling it up to a total volume of 10 ml.
3. Vortex the container to ensure thorough mixing of the reagents.
4. Cover the surface where the gel is intended to be with the mixture and let it remain in contact for 10 minutes (or 1 hour for larger objects).
5. Rinse the surface twice with Ethanol 96% to remove any residue.
6. Allow the surface to air dry completely.

Gel Bulk

1. Prepare an Eppendorf tube and add the following reagents in the specified order, check the quantities indicated in the table below:
   a) PBS
   b) 40% Acrylamide
   c) 2% BisAcrylamide
2. Gently mix the contents of the Eppendorf tube by pipetting up and down.
3. Perform a short spin.
4. Add the following reagents in the given order, again, check the quantities indicated in the table below:
   a) Beads
   b) APS
   c) TEMED
5. Mix the contents of the Eppendorf tube by pipetting up and down using a P1000 pipette.
6. For 12mm glass coverslips, add a drop of 10 µl of the mixture. For 18mm glass coverslips, add a drop of 22 µl. For glass sandwiches, add a minimum of 40 µl (adjust accordingly if they are too thin).
7. Place a glass coverslip on top of the drop and allow the mixture to polymerize for 40 minutes.

8. After polymerization, immerse the sample in PBS for a couple of minutes.
9. Using tweezers, carefully detach the glass coverslip from the gel.

Gel coating

1. Prepare an Eppendorf tube and add the following reagents in the specified order:
   a) 50 µl of HEPES 0.5M pH 6.
   b) 0.5 µl of Bis at 2% (or 5 µL Bis at 0.2%).
   c) 1.5 µl of NHS/DMSO 10 mg/ml (variable [2.5 0.25]).
   d) 5 µl of Irgracure (5 mg/ml in 70% ethanol).
   e) 3 µl of Tetracrylate 0.2% in milliQ water.
   f) 440 µl of milliQ water to reach a total volume of 500 µl.
2. Cover the gels with 40 µl for 12mm gels or 80 µL for 18mm gels.
3. Place a glass coverslip on top of the gel.
4. Expose the sample to UV light for 5 minutes to initiate polymerization.
5. Wash the gel twice with HEPES 25 mM pH 6, performing quick washes.
6. Wash the gel twice with PBS, performing quick washes.
7. Place a drop of the protein mixture on top of the gel. The protein mixture consists of 10 µL of fn (fibronectin) in 990 µl of PBS.
8. Leave the sample overnight in the refrigerator.
9. Wash the gel three times for 5 minutes each with PBS, ensuring thorough drying between washes.
10. Cells can now be seeded on top of the prepared gel for further experiments.

N.S. (KPa)	**0.5**	**1.5**	**2**	**3**	**5**	**11**	**18**	**30**	**150**
M.S. (Pa)	0.64	1.50	2.37	3.40	5.26	10.94	16.80	29.92	136.10
Acrylamide 40%	50	62.5	68.75	77	93.3	93.75	94.4	150	150
BisAcrylamide 2%	7.5	10	11	11	11	25	40	37.5	150
Beads	8	8	8	8	8	8	8	8	8
APS	2.5	2.5	2.5	2.5	2.5	2.5	2.5	2.5	2.5
TEMED	0.25	0.25	0.25	0.25	0.25	0.25	0.25	0.25	0.25
PBS	429.75	414.75	407.5	399.25	382.95	368.5	352.85	299.75	187.25
Final Volume	500	500	500	500	500	500	500	500	500

Annex 6: Fixation and Immunocytochemistry

Fixation of cells Protocol

1. Rinse the cells twice with warm PBS for a duration of 3 minutes each.
2. Fix the cells by treating them with 4% PFA for 12 minutes at room temperature (RT) in darkness.
3. Wash the cells with PBS two additional times to remove any residual PFA.
4. Finally preserve the fixated cells in a 4-degree refrigerator.

Immunocytochemistry protocol

1. Wash the samples with PBS.
2. Wash the samples with 0.1% Triton X100 in PBS for 10 minutes at RT.
3. Incubate the samples with 2.5% BSA in PBS for 30 minutes at RT.
4. Add the primary antibody in FG-PBS, covering the gel or well with 100 µl of the solution. Incubate at RT for 1.5 hours or alternatively at 4°C overnight.
5. Wash the samples three times with PBS for 3 minutes each.
6. Incubate the samples with the secondary antibodies diluted in PBS (1:500) along with Hoechst 33342 DNA stain at a 1:1000 dilution for 1 hour at RT.
7. Wash the samples three times with PBS for 3 minutes each.
8. If mounting is required, allow the samples to dry and apply Mowiol. Leave them to dry overnight at RT.
9. The following day, the samples can be imaged or stored at 4°C.